UNIVERSIDADE DE LISBOA
FACULDADE DE CIÊNCIAS
DEPARTAMENTO DE BIOLOGIA VEGETAL

Crosstalk between the miRNA and the SnRK1 signalling pathways

Diana Reis Barata

Mestrado em Biologia Molecular e Genética

Dissertação orientada por:
Doutora Elena Baena-González
Professor Doutor Jorge Silva

2018

ACKNOWLEDGEMENTS

First of all, I want to thank Elena Baena for giving me the opportunity of working in the Plant Stress Signalling (PSS) group. It was an incredible journey and it was such an honour to meet and work with you. You're so enthusiastic about science and your work is remarkable. You're the kind of person whose thoughts are always running in high speed through your head, trying to connect dots between loose ends and you always have a question in mind that helps us finding new and better ways to achieve results. Thank you so much for all the support, motivation and knowledge transmitted during this period.

I would also like to thank my Professor, Jorge Silva, for accepting to be my co-supervisor and for all shown availability and help during this thesis.

My dear Ana Confraria, I was so blessed to have you as my mentor. You are amazing!! Thank you for your patience (I acknowledge that it's necessary lots of it to teach me), for your kindness and dedication and for guiding me and boosting my confidence in the lab. You are such a smart girl! You are optimistic, perfectionist, humble, extremely focused and you even manage to be really funny. One day I aspire to be a researcher just like you! "Obrigada" é uma palavra demasiado pequena para expressar o quão grata me sinto por tudo o que me tens ensinado.

To all the other PSS members, Leonor, Mattia, Alex, Américo and Borja, thank you for all the knowledge shared, for helping me whenever I had questions and doubts and for all the amusing moments in the lab. I wish to also thank our lab neighbours, the Plant Molecular Biology group, for sharing knowledge, experience and lab material. A special thank to Rui and Pipa, for all the support and for your priceless friendship.

To Vera, our plant technician, and my 10-years-apart twin sister, for taking such a great care of our plants and plant growth facilities. Thank you also for the laugher moments and for your accurate sense of humour.

Last but not least, I would like to acknowledge my friends, my parents, my sister and my boyfriend. They were a fundamental piece in this chapter of my life. Their support was invaluable!

Obrigada à minha mãe, ao meu pai, à minha irmã, ao Jota e aos meus amigos do coração pelas oportunidades que me deram e por porem sempre o meu bem-estar na primeira linha das suas prioridades. Obrigada pelo carinho, por tomarem conta de mim nos momentos mais difíceis, por me encorajarem a perseguir uma carreira e por acreditarem em mim.

ABSTRACT

As sessile organisms, plants are constantly exposed to environmental stresses that limit photosynthesis and/or respiration, thereby compromising ATP production, growth, and ultimately survival. To cope with these conditions, plants have evolved mechanisms that promote stress and defence responses at the expense of growth until the environmental conditions become favourable again.

A core component of stress signalling pathways is the evolutionarily conserved sucrose non-fermenting 1 (SNF1)-related protein kinase 1 (SnRK1), the plant ortholog of yeast SNF1 and mammalian AMP-activated protein kinase (AMPK). SnRK1 is activated in response to declining energy levels during stress, implementing a vast metabolic and transcriptional reprogramming that restores homeostasis and thereby promotes plant survival.

How SnRK1 regulates gene expression, and in particular how it exerts gene repression is poorly understood, but several lines of evidence suggest the involvement of microRNAs (miRNAs) in this process. miRNAs are 20–24nt non-coding RNAs that regulate gene expression posttranscriptionally mainly through cleavage and/or translation repression of complementary mRNA targets. MiRNAs have been extensively implicated in plant growth and development, but also in responses to environmental stress. SnRK1 has been shown to repress particular targets in a miRNA-dependent manner, suggesting that SnRK1 and miRNAs signalling pathways may be interconnected, even though the mechanisms underlying this connection are currently unclear.

The aim of this thesis was to explore the mechanisms underlying this crosstalk by testing two non-mutually exclusive hypotheses: a) SnRK1 affects miRNA biogenesis and b) SnRK1 affects miRNA activity.

To test the first hypothesis, I compared the levels of two specific miRNAs, miR156 and miR319, between wild-type *Arabidopsis* plants and SnRK1 partial loss-of-function mutants. Results showed that the partial inactivation of SnRK1 is accompanied by reduced levels of both miRNAs, suggesting that SnRK1 may be required for miRNA accumulation.

To address whether SnRK1 affects miRNA activity and based on preliminary results from the Baena-González Lab, I asked whether SnRK1 could interact with ARGONAUTE 1 (AGO1), the major effector of the RNA-induced silencing complex (RISC). MiRNA activity is dependent on the correct loading of mature miRNAs into appropriate AGO proteins. In *Arabidopsis*, there are ten members of the AGO family, but most miRNAs are loaded into AGO1. I started by testing for a physical interaction between SnRK1 and AGO1 using yeast-two-hybrid (Y2H) pairwise assays, followed by co-immunoprecipitation from plant extracts. Results showed that SnRK1α1 physically interacts with AGO1 in yeast; on the other hand, by co-immunoprecipitation I was unable to detect *in planta* interactions between SnRK1α1 and AGO1 in mature leaves. However, to confidently discard or confirm a physical interaction *in planta*, it would be important to repeat the co-immunoprecipitation in tissues or conditions with higher AGO1 expression and, eventually, to optimise further the co-immunoprecipitation conditions.

In parallel, I asked whether there were genetic interactions between AGO1 and SnRK1. For that, *ago1-27* mutants were crossed to SnRK1α1 loss- and gain-of-function mutants and their genetic interaction was evaluated using both a phenotypic characterisation of early seedling development under increasingly high concentrations of glucose or ABA and a flowering time assessment in long day conditions. Regarding seedling development, *ago1-27* enhances the hypersensitivity of the SnRK1α1 overexpressor (OE) to stress derived from high concentrations of glucose, whilst under high

concentrations of ABA, SnRK1α1OE enhances the hypersensitive phenotype of *ago1-27*, suggesting that AGO1 and SnRK1 may negatively regulate each other. Moreover, the SnRK1 pathway seems to predominate under high sugar stress whilst AGO1 seems to be more important for ABA responses. Interestingly, the *snrk1α1-3* mutation partially reverted the delayed flowering phenotype of *ago1-27*, further reinforcing that AGO1 is a negative regulator of SnRK1.

Finally, to explore the functional interaction between SnRK1 and AGO1 in the future, I developed important genetic tools based on a *SUC::SUL* reporter line that will allow to test whether changes in SnRK1 levels and activity affect AGO1-mediated silencing activity. The *SUC::SUL* reporter is based on the vasculature-specific silencing of a gene involved in chlorophyll biosynthesis (*SULPHUR*), through small interfering RNAs derived from its sense and antisense expression under the *SUC2* promoter. New plant lines for different *snrk1α* mutants harbouring this reporter were generated and are ready to be used in future assays, for which the experimental setup was also optimised here.

Taken together, the results presented in this thesis suggest that SnRK1 may indeed regulate the miRNA pathway at different levels, affecting miRNA accumulation and potentially AGO1 function to control growth, development and plant stress responses. Further work will be required to confirm the extent and mechanism by which SnRK1 impacts on miRNA biogenesis and/or stability and to dissect the details of its interaction with AGO1.

KEYWORDS: SnRK1; miRNAs; AGO1; *Arabidopsis thaliana;* Environmental stress

RESUMO ALARGADO

As plantas, devido à sua incapacidade de locomoção, estão confinadas ao local onde germinaram sendo, por isso, vulneráveis a condições ambientais que restringem o seu crescimento e desenvolvimento. Temperaturas extremas, seca, inundações, elevada salinidade, exposição a metais pesados, lesões mecânicas, condições de luz inadequadas e infeção por patogéneos estão entre as maiores causas de perda de produtividade agrícola a nível mundial.

Para fazer face a estas flutuações ambientais, as plantas desenvolveram, por um lado, estratégias adaptativas de sobrevivência de carácter específico, que lhes permitem responder a um tipo particular de stress e, por outro, mecanismos gerais responsáveis pelo ajuste metabólico e pela reprogramação da expressão de genes, permitindo, assim, rapidamente reparar os componentes celulares danificados e alocar nutrientes para os processos adequados, de forma a restaurar a homeostasia.

Em condições normais, as plantas convertem a luz em energia química sob a forma de açúcares que são depois distribuídos pelos vários órgãos da planta permitindo o seu correto crescimento e desenvolvimento. Contudo, condições desfavoráveis com impacto deletério nos processos de fotossíntese e respiração resultam, frequentemente, na diminuição dos níveis de energia celular da planta e afetam a alocação de açúcares para os órgãos em crescimento, levando à ativação da proteína cinase SnRK1. Esta, por sua vez, para restabelecer a homeostasia, ativa processos catabólicos e inibe processos anabólicos através da fosforilação de diversas enzimas metabólicas e de uma extensa reprogramação do transcriptoma, permitindo, assim, a aclimatação e sobrevivência das plantas.

A SnRK1 pertence a uma família altamente conservada de cinases e partilha semelhanças estruturais e funcionais com as proteínas ortólogas "AMP-activated protein kinase" (AMPK), nos mamíferos, e "Sucrose non-fermenting 1" (SNF1), nas leveduras, funcionando como um complexo heterotrimérico composto por uma subunidade catalítica α e duas subunidades regulatórias, β e γ. Em *Arabidopsis*, existem três diferentes isoformas de SnRK1α, apesar de apenas duas (codificadas pelos genes *SnRK1α1/KIN10* e *SnRK1α2/KIN11*) serem expressas constitutivamente em todos os tecidos da planta, três diferentes isoformas de SnRK1β (codificadas pelos genes *SnRK1β1*, *SnRK1β2* e *SnRK1β3*) e apenas uma isoforma da subunidade γ, SnRK1βγ.

Não obstante a sua enorme importância a nível da resposta a diferentes tipos de stress, a via de sinalização da SnRK1 vai além do mero ajuste metabólico nessas condições, estando igualmente implicada na sinalização de açúcares, associada a vias de sinalização mediadas por várias hormonas vegetais e envolvida na modulação do crescimento e desenvolvimento das plantas.

Contudo, apesar do seu papel central, são poucos os mecanismos descritos, até à data, capazes de explicar a reprogramação transcripcional desencadeada pela SnRK1. O aumento da expressão de determinados genes, por seu lado, é atribuído em grande parte a fatores de transcrição "basic leucine Zipper" (bZIP) bem estabelecidos enquanto efetores a jusante da via de sinalização da SnRK1. Por outro lado, quanto à repressão de genes, os mecanismos subjacentes continuam maioritariamente desconhecidos, embora os microRNAs (miRNAs) tenham sido implicados na repressão de alguns dos alvos de SnRK1, ainda que através de mecanismos desconhecidos.

Os miRNAs correspondem a uma classe de pequenos RNAs endógenos não codificantes com 20-24 nucleótidos que regulam a expressão de genes pós-transcricionalmente, através da clivagem e/ou do bloqueio da tradução de transcritos complementares. Desta forma, os miRNAs têm sido extensivamente implicados tanto no crescimento e desenvolvimento das plantas como na resposta a fatores de stress biótico e abiótico.

O trabalho desenvolvido nesta tese de mestrado teve como principal objetivo aumentar o conhecimento sobre os mecanismos envolvidos na comunicação entre a via de sinalização de SnRK1 e os miRNAs. Para isso, foram testadas duas hipóteses não mutuamente exclusivas: a) SnRK1 afeta a biogénese de miRNAs e b) SnRK1 afeta a atividade de miRNAs.

A biogénese de miRNAs ocorre no núcleo, englobando várias processos interdependentes desempenhados por componentes organizados num complexo. Em linhas gerais, a RNA Polimerase II (Pol II) é recrutada para o gene *MIR*, promovendo a sua transcrição e dando origem a um miRNA primário (pri-miRNA) que é processado pela proteína "DICER-like 1" (DCL1) com o auxílio das proteínas "Hyponastic-leaves 1" (HYL1) e "Serrate" (SE), originando um percursor de miRNA (pré-miRNA). Este pré-miRNA é novamente processado pela DCL1, originando uma pequena cadeia dupla formada por miRNA/miRNA*, que constituem respectivamente a cadeia guia e a cadeia passageira. A extremidade 3' do duplex miRNA/miRNA* é metilada pela metil-transferase "Hua-Enhancer 1" (HEN1). Ainda no núcleo, a cadeia passageira é normalmente alvo de degradação e a cadeia guia, que constitui o miRNA maduro, é reconhecida e incorporada no complexo "RNA-induced Silencing Complex" (RISC). Este complexo tem como principal efetor uma proteína da família "ARGONAUTE" (AGO), responsável pelo reconhecimento, já no citoplasma, de transcritos-alvo com sequência complementar à do miRNA, e pela sua subsequente clivagem ou bloqueio de tradução.

Problemas na biogénese de miRNAs refletem-se, normalmente, num aumento de pri-miRNAs e numa acumulação deficiente de miRNAs maduros. Deste modo, para testar a primeira hipótese, comecei por analisar a acumulação de dois miRNAs específicos – miR156 e miR319 – em plantas *Arabidopsis* tipo silvestre e em mutantes com perda parcial de função de SnRK1. Os resultados mostraram que a inativação parcial de SnRK1 levou à redução dos níveis de expressão de ambos os miRNAs testados. Ainda que não se consiga apurar por agora se este é um efeito específico para os miRNAs testados ou se se trata de um mecanismo geral, a confirmar-se futuramente estes mesmos resultados para outros miRNAs, pode potencialmente significar que a atividade de SnRK1 é uma condição necessária para a correta acumulação de miRNAs.

Para perceber se SnRK1 afeta a atividade de miRNAs, e com base em resultados preliminares do laboratório da Baena-González, procurei avaliar se SnRK1 poderia eventualmente estar a interagir com a proteína AGO1, o maior efector do complexo de silenciamento RISC. O correto reconhecimento dos miRNAs pela proteína AGO adequada e a sua subsequente incorporação no complexo RISC representa a etapa final da biogénese de miRNAs e é crítico para a sua interação com os respetivos transcritos-alvo. Em Arabidopsis, a família AGO é constituída por dez membros, mas os miRNAs são, na sua grande maioria, incorporados na AGO1. Assim, comecei por testar a interação física entre SnRK1 e AGO1 através de ensaios par-a-par de dois híbridos em levedura ("Yeast Two Hybrid" - Y2H) seguido de uma co-imunoprecipitação. Apesar de ter sido detetada uma interação positiva entre SnRK1α1 e AGO1 em levedura, através da co-imunoprecipitação não foi possível detetar interações entre as duas proteínas *in planta* em folhas maduras de roseta. Este resultado poderá ser talvez devido ao carácter transiente ou fraco da interação ou à sua ocorrência específica em determinados tecidos ou fases de desenvolvimento. No futuro, seria importante repetir esta experiência em tecidos ou condições em que a expressão de AGO1 seja mais elevada, eventualmente, otimizando ainda as condições da co-imunoprecipitação, para que se possa confiantemente descartar ou confirmar a ocorrência de interação física entre SnRK1 e AGO1 *in planta*.

Paralelamente a esta abordagem bioquímica, procurei ainda perceber se existia alguma interação genética entre AGO1 e SnRK1. Para tal, mutantes *ago1-27*, deficientes no silenciamento pós-translacional de genes, foram cruzados com mutantes com ganho e perda de função de SnRK1α1. A

interação genética foi avaliada com base na caracterização fenotípica dos processos de germinação e enverdecimento dos cotilédones na presença de elevados níveis de glucose ou ácido abscísico (ABA) e com base no tempo de floração em condições de dias longos. Relativamente à germinação e enverdecimento dos cotilédones, enquanto que, sob elevados níveis de glucose, a mutação *ago1-27* parece potenciar a hipersensibilidade do sobreexpressor de SnRK1α1, sob elevadas concentrações de ABA é o sobreexpressor de SnRK1α1 que parece aumentar o fenótipo hipersensível do mutante *ago1-27*. Estes resultados sugerem uma possível regulação negativa de AGO1 sobre SnRK1 e *vice-versa* cuja intensidade e sentido podem variar consoante o tipo de stress. Curiosamente, a mutação *snrk1α1-3* reverteu parcialmente o fenótipo de floração atrasado do mutante *ago1-27*, com o duplo mutante a florir em média dois dias antes do que as plantas *ago1-27* e com menos folhas de roseta do que as plantas do tipo silvestre, reforçando ainda mais o potencial papel de AGO1 enquanto regulador negativo de SnRK1.

Finalmente, para explorar a interação funcional entre SnRK1 e AGO1, desenvolvi importantes ferramentas genéticas baseadas numa linha repórter *SUC::SUL* que irão permitir, no futuro, testar até que ponto diferentes níveis de SnRK1 influenciam a atividade silenciadora de AGO1. No sistema repórter *SUC::SUL*, um RNA de cadeia dupla do gene *SULPHUR*, é expresso sob o controlo do promotor *SUC2*, específico das células de companhia do floema, dando origem a pequenos RNAs de interferência que são incorporados na AGO1, reprimindo, assim, o transcrito *SUL* (envolvido na biossíntese de clorofila) e causando a clorose das células silenciadas na vasculatura. Novas linhas de plantas homozigóticas para este repórter contendo diferentes mutações das subunidades catalíticas de SnRK1 foram geradas e estão prontas para ser usadas em ensaios futuros para os quais a configuração experimental foi também aqui otimizada.

Em suma, os resultados apresentados nesta tese fornecem novas evidências que apontam para uma possível ação de SnRK1 em diferentes níveis de regulação sobre a via de sinalização dos miRNAs, nomeadamente na acumulação de miRNAs e na atividade de AGO1, para controlar o crescimento, desenvolvimento e respostas das plantas a stress. Estudos futuros serão necessários para confirmar a extensão e mecanismo de impacto de SnRK1 na biogénese de miRNAs e para dissecar em detalhe a interação com AGO1.

PALAVRAS-CHAVE: SnRK1; miRNAs; AGO1; *Arabidopsis thaliana;* Stress ambiental

TABLE OF CONTENTS

INDEX OF FIGURES

INDEX OF TABLES

ABBREVIATION LIST

ABA	Abscisic acid
AGO1	ARGONAUTE1
AMPK	AMP-activated protein kinase
bZIP	Basic leucine Zipper
DCL1	DICER-like 1
HEN1	HUA-ENHANCER 1
HYL1	HYPONASTIC LEAVES 1
KO	Knockout
mRNA	Messenger RNA
miRNA	MicroRNA
Pol II	RNA Polymerase II
pre-miRNA	Precursor miRNA
pri-miRNA	Primary miRNA
SE	SERRATE
siRNA	Small interfering RNA
SNF1	Sucrose non-fermenting 1
SnRK1	Sucrose non-fermenting 1-related protein kinase 1
sRNA	Small RNA
RISC	RNA-induced silencing complex
RNA	Ribonucleic Acid
WT	Wild-type
Y2H	Yeast-two-hybrid

I. INTRODUCTION

1. Environmental stress and SnRK1 activation

As sessile organisms, plants are constantly exposed to changing environmental conditions that threaten homeostasis, fitness and ultimately plant survival. Extreme temperatures, drought, flooding, high salinity, exposure to heavy metals, mechanical wounding, inadequate light conditions and infection by pathogens are amongst the major causes of crop losses worldwide[1].

To cope with these conditions, plants rely on stress-specific mechanisms that promote tolerance to particular types of stress, such as the induction of a specific Na^+ transporter to extrude salt from tissues[2] or the induction of localised cell death in the root cortex to promote airflow and respiration during flooding[3]. However, general mechanisms that reprogram metabolism and gene expression are also essential to mount a successful stress response by allowing the repair of damaged cellular components, the redistribution of resources to appropriate processes, and ultimately by restoring homeostasis[4].

One important general stress signal is the depletion of cellular energy. Under normal conditions, plants convert light into chemical energy in the form of sugars, which then need to be distributed throughout the different organs to allow proper growth and development. However, hostile conditions often lead to reduced rates of photosynthesis and/or respiration, affecting the overall energy status of the plant, the allocation of sugars to the growing organs, and ultimately limiting growth and development[5,6].

When ATP production is compromised and carbon levels decline, the energy sensing Snf1-related protein kinase 1 (SnRK1) is activated. To re-establish homeostasis, SnRK1 turns on energy-producing processes and inhibits energy-consuming pathways through a vast transcriptional reprogramming and through phosphorylation of a number of metabolic enzymes, thus promoting stress tolerance and survival[7–9].

2. SnRK1 structure and function

SnRK1 belongs to a family of evolutionarily conserved kinases and shares structural and functional features with its ortholog proteins, the mammalian AMP-activated protein kinase (AMPK) and the yeast Sucrose non-fermenting 1 (Snf1)[10]. It functions as a heterotrimeric complex composed by a catalytic α subunit and two regulatory subunits, β and γ.

The α subunit comprises a catalytic domain harbouring a conserved T-loop whose phosphorylation is essential for activity, and a regulatory domain that is important for the interaction with the β and γ subunits. The β subunit regulates subcellular localization and kinase activity and acts as a scaffold between α and γ subunits[9,11,12]. In mammals AMP and ADP bind to the AMPK γ subunit, thereby stimulating T–loop phosphorylation and activation of AMPK[13,14]. In plants, however, the only γ-like subunit present in SnRK1 heterotrimeric complexes is the highly atypical βγ, which does not appear to bind AMP or ADP[15,16].

In *Arabidopsis*, there are three different SnRK1α isoforms [encoded by the *SnRK1α1/KIN10*, *SnRK1α2/KIN11* and *SnRK1α3/KIN12* genes – although *SnRK1α3* is poorly expressed in most plant tissues)[17] and three different SnRK1β isoforms (encoded by the *SnRK1β1*, *SnRK1β2*, *SnRK1β3* genes), whereas SnRK1βγ is encoded by a single gene. Given this, it is likely that different SnRK1 αβγ heterotrimers assemble through various combinations of α1/α2/β1/β2/β3/βγ subunits and that

consequently SnRK1 complex composition may differ between particular subcellular compartments, tissues or developmental stages[9]. The number of possible combinations is further increased when considering that most SnRK1 transcripts can be alternatively spliced.

A complete SnRK1α1/α2 knockout is lethal in higher plants[7] and plants with compromised SnRK1 function display several metabolic and developmental defects, such as defective seed storage, maturation and dormancy in pea[18], male sterility in barley[19], and impaired starch degradation, severe growth reduction, and early senescence in *Arabidopsis*[7]. Moreover, antisense mediated silencing of the β-subunit StubGAL83 in potato, affects tuber and root development[20]. Conversely, SnRK1α1 overexpression in *Arabidopsis* delays flowering and senescence, alters significantly seedling growth, and promotes tolerance to stresses such as nutrient-deprivation or hypoxia[21,22].

In brief, SnRK1 functions as a sugar signalling hub, being activated under carbon starvation and inhibited by sugars like trehalose-6-phosphate (T6P)[23,24] by mechanisms not yet fully understood[9]. Supporting the regulation of SnRK1 by the carbon status, SnRK1α1 overexpression generates a starvation transcriptomic signature opposite to that occurring in response to supply of exogenous sugar[7].

The SnRK1 pathway has also been shown to interact with several hormonal pathways. Leaf senescence driven by ethylene signalling is in part regulated by the SnRK1-mediated repression of the transcription factor ETHYLENE INSENSITIVE3 (EIN3)[25]. A physical interaction between SnRK1α1 and MYC2, a master regulator of jasmonate (JA) signalling, has also been established[26]. Importantly, SnRK1 connection to abscisic acid (ABA) signalling has been demonstrated through phenotypical and biochemical analyses of SnRK1 mutants[27] and further supported by the identification of two established repressors of the ABA pathway (ABI1 and PP2A) as negative regulators of SnRK1 signalling[28].

SnRK1 implements vast metabolic changes during stress, partly through the direct phosphorylation of biosynthetic enzymes such as sucrose phosphate synthase (SPS)[29,30], HMG-CoA reductase (HMGR)[29], nitrate reductase (NR)[29,30], 6-phosphofructo-2-kinase/2,6-fructose-bis-phosphatase (F2KP)[31] and trehalose-6-phosphate synthase (TPS)[30,32].

On the other hand, SnRK1 also induces an extensive transcriptional reprogramming through mechanisms mostly still unknown. bZIP transcription factors are well described in the literature as downstream effectors of the SnRK1 signalling cascade in response to low-energy stress, salt stress, or during dark-induced senescence[7,33,34], but other factors involved in SnRK1-dependent gene regulation, and in particular in gene repression, remain largely unidentified.

In the last decade, miRNAs have been increasingly implicated in the response to environmental stress[35] and previous work from the Plant Stress Signalling Group has shown that miRNAs can mediate the repression of specific mRNA targets by SnRK1 in response to energy deprivation[36]. Nevertheless, the underlying mechanisms remain elusive.

3. miRNAs and ARGONAUTE1

MicroRNAs (miRNAs) are a class of endogenous non-coding 20- to 24-nucleotide RNAs involved in post-transcriptional gene repression. In plants, miRNAs act either through cleavage or translation attenuation of complementary mRNA targets[37].

In Arabidopsis, miRNAs biogenesis takes place in the nucleus through a series of interdependent steps involving cooperation of several proteins. More specifically, RNA Polymerase II (Pol II) is recruited

to the promoters of *MIR* genes, transcribing them into primary-miRNAs (pri-miRNAs)[38]. Then, pri-miRNAs fold into stem-loop structures that are processed through cleavage by DICER-LIKE 1 (DCL1) into miRNA precursors (pre-miRNAs). In this first step, central components like HYPONASTIC LEAVES1 (HYL1) and SERRATE (SE) interact and collaborate with DCL1 to promote the accurate processing of pri-miRNAs[39]. Pre-miRNAs are further processed by DCL1 into miRNA/miRNA* duplexes that are stabilised through 3´-terminal 2´-O-methylation by HUA ENHANCER 1 (HEN1)[40]. Recent evidence suggests that, while in the nucleus, mature miRNAs (miRNA single guide strands) are recognised and loaded into the RNA-induced Silencing Complex (RISC) containing ARGONAUTE1 (AGO1) proteins[41]. The passenger strands (miRNAs*) are often targeted for degradation and the miRNA-loaded RISC complexes are exported to the cytoplasm where AGO1 recognises target mRNAs complementary to the loaded miRNA, either slicing the transcript or blocking its translation[42–49].

Mutations that compromise the function of the miRNA biogenesis machinery or the RISC complex often lead to aberrant plant phenotypes with pleiotropic developmental defects, such as abnormal embryogenesis, short stature, altered leaf shape, defects in floral meristems and reduced fertility[50–52], reinforcing the importance of these small RNAs as crucial developmental regulators.

Well-known examples of this are miR156 and miR172, two independent but interconnected miRNAs involved in flowering time control, whose expression levels are oppositely correlated[53]. Other examples include miR319, which targets *TEOSINTE BRANCHED1*, *CYCLOIDEA*, and *PROLIFERATING CELL NUCLEAR ANTIGEN BINDING FACTOR* (TCP) transcription factors that regulate leaf shape and senescence[54], miR159, which targets MYB transcription factors with a role in seed germination[55] and miR396, which targets *GROWTH-REGULATING FACTORs (GRF)* involved in the regulation of cell division[56].

Besides their established role in plant growth and development, miRNAs are also involved in the response to multiple stresses[57]. For example, in *Arabidopsis*, miR160 promotes tolerance to heat stress[58] and miR394 acts as a negative regulator of resistance to *Botrytis cinerea*[59]. Additionally, the expression levels of several miRNAs are differentially influenced by distinct types of stress, sometimes, in a tissue-dependent manner. In *Arabidopsis*, the expression of miR169 increases upon exposure to salt[60] but decreases during drought treatment[61] and, in wheat, at least six miRNAs, including miR159, miR172, miR319, miR399, miR528, and miR4393 showed an induced expression in leaves but were inhibited in roots, in response to drought[62]. Moreover, miRNA biogenesis mutants are often hypersensitive to ABA, a key regulator of abiotic stress tolerance, and display aberrant responses to different types of stresses, including salt and osmotic stress[63–66].

Over the past years many factors involved in miRNA signalling have been discovered, suggesting that miRNAs are tightly regulated at several levels, such as transcriptional induction, splicing, processing, loading, export, activity and degradation[37,67].

The precise recognition of miRNAs by the appropriate ARGONAUTE protein and their subsequent loading to the RISC complex represents the final step of miRNA biogenesis and is critical for their interaction with targets. In Arabidopsis, the ARGONAUTE family comprises 10 member proteins, all harbouring N-terminal, PAZ, MID and PIWI domains[68], and the sorting of each miRNA into a specific AGO relies mainly, but not exclusively[69], on the identity of the 5'-sequence position of mature miRNAs[70–72]. From the 10 AGO family members, ARGONAUTE 1 is particularly important since the majority of the mature miRNAs are sorted into it, given their 5’-terminal uridine. By contrast, miRNAs bearing a 5’ terminal adenosine are preferentially loaded into AGO2 whereas those carrying

a cytosine at the 5' terminus are sorted to AGO5[70,72,73].

AGO1 is a nucleo-cytosolic shuttling protein[41] with slicer activity that selectively recruits miRNAs for post-transcriptional gene silencing (PTGS)[74], being able to regulate its own expression *via* a negative feedback loop that involves miR168 activity[75].

In addition to its well-described role in PTGS, AGO1 was recently implicated in the co-transcriptional down-regulation of *MIR* genes[67] and in the transcriptional induction of jasmonate signaling genes through direct chromatin binding at the target loci[76].

Given the importance of SnRK1 signalling for stress tolerance and the increasing number of reports linking miRNAs to stress responses, the Baena-González group proposed a possible cross-talk between these two pathways. The finding that the repression of specific transcripts by SnRK1 requires miRNAs confirmed this hypothesis, establishing miRNAs as downstream effectors of SnRK1 signalling[36]. However, the mechanisms by which SnRK1 affects miRNA signalling pathways remained unknown.

Therefore, the aim of this thesis was to gain mechanistic insight into how SnRK1 activity results in miRNA-mediated gene repression. To this end, two non-mutually exclusive hypotheses were tested: a) SnRK1 affects miRNA biogenesis and b) SnRK1 affects miRNA activity, possibly through an interaction with AGO1.

II. MATERIALS AND METHODS

A list of all primers used in this study is provided in Table S1.

1. Plant material and growth conditions

All *Arabidopsis thaliana* plants used are in the Columbia (Col-0) background except *35S::SnRK1α1-HA*, which is in Landsberg erecta[7]. The *snrk1α1-3*[33], *35S::SnRK1α1*[27], *snrk1α2-1*[77], *ago1-27*[78] and *SUC::SUL* plant lines[79,80] have been previously described. *snrk1α2-2* is a T-DNA insertion mutant (WiscDsLox384F5), which had been previously isolated and preliminarily characterised in the Baena-González lab (A. Confraria, unpublished). These single mutants had previously been crossed to generate partial SnRK1α loss-of-function mutants (*snrk1α1*$^{-/-}$ *snrk1α2*$^{+/-}$ and *snrk1α1*$^{+/-}$ *snrk1α2*$^{-/-}$; A. Confraria, unpublished), hereafter designated as *sesquiα2* and *sesquiα1,* respectively, depending on the *snrk1α* mutation that is segregating. For plant growth seeds were surface-sterilised for 1 min in 70% (V/V) ethanol followed by 10 min in 20% (V/V) bleach under gentle rocking, and then washed at least 3 times in sterile water. Sterilised seeds were stratified in the dark at 4°C for 2-3 days and sowed on plates containing half strength Murashige and Skoog medium (Duchefa Biochemie) with 0.1% MES and 0.8% phytoagar. Unless otherwise specified, plants transferred to soil were grown under a 16h-light (100µmol m^{-2} s^{-1}), 22ºC / 8h-dark, 18ºC regime.

2. RNA extraction and cDNA synthesis

Total RNA was extracted from rosette leaves of 5 week-old plants grown in soil under a 12h-light (110 µmol m^{-2} s^{-1}, 22ºC)/12h-dark (18ºC) regime with TRIzol™ (ThermoFisher Scientific) according to the manufacturer's instructions. RNA was then treated with RQ1 RNase-Free DNase (Promega; 2 DNase units per µg of RNA) at 37°C for 30 min and recovered by a phenol/chloroform extraction and subsequent precipitation with isopropanol. DNase-treated RNA (1 µg) was reverse transcribed in a total reaction volume of 40µL using Super Script III Reverse Transcriptase (InvitrogenTM), following the manufacturers' instructions. cDNA was synthesised using a mix of OligoDT (for the housekeeping genes) and miRNA-specific primers (**Supplementary Table 1**).

3. Quantitative real-time RT-PCR (RT-qPCR)[81]

qRT-PCR analyses were performed in 384-well reaction plates using the QuantStudio™ 7 Flex Real-Time PCR System (Thermo Fisher). The reactions were prepared in a total volume of 10µL containing 1µL of cDNA (diluted 1:10) corresponding to 2.5ng of RNA, 5µL of iTaq Universal SYBR Green Supermix (BioRad) and 0.8µL of each gene-specific 5µM primer. No-template and -RT controls were included for each gene in comparative gene expression analyses.

The $2^{-\Delta\Delta Ct}$ method was used for relative quantification[82]. Expression values were normalised to the geometric mean of Ct values obtained for the following reference genes: *EIF4* (At3g13920), *UBQ10* (At4g05320) and *UBC21* (At5g25760)[83].

4. Plasmid construction and Yeast-two-hybrid assay

The full *AGO1* coding sequence was amplified from the plasmid pHBT95-AGO1 already existing in the Baena-González lab, using primers containing attB1 and attB2 sites. The PCR product was extracted and purified from a 0.8% agarose-TAE gel, using a Macherey-Nagel NucleoSpin® Gel and PCR Clean-up, following the manufacturer's instructions. The purified PCR product was thereafter recombined into the pDONR221 vector through a BP reaction. Recombination and incorporation of

the *AGO1* insert into the pDONR221 vector was further confirmed using two restriction enzymes – XbaI and BamHI – to digest the resultant pENTR clones and the full-length *AGO1* insert was sequenced to confirm the absence of PCR-derived mutations. This entry clone was then recombined by an LR reaction into a Gateway™-modified pGADT7 destination vector (pDEST-GADT7) kindly provided by Nasser Rusan (NIH, Maryland, USA) and the recombination sites flanking *AGO1* were sequence-verified before proceeding to the next step. All SnRK1 subunits (α1, α2, β1, β2, β3 and βγ), cloned into pGBKT7 vectors, were already available in the Baena-González lab.

Competent yeast cells (Y2HGold) were co-transformed with pDEST-GADT7-AGO1 and pGBKT7 vectors containing the SnRK1 subunits. Each construct was also co-transformed with the complementary empty vector, to control for growth due to auto-activation. Three independent colonies of each co-transformation were inoculated into liquid synthetic dropout (SD) medium and grown to saturation, at 28ºC, shaking at 180rpm. Ten-fold serial dilutions of saturated yeast cultures were spotted onto plates containing SD medium with increasing stringency, lacking 3 (-L-W-H) or 4 (-L-W-H-A) amino acids. When indicated, 25 mM amino-triazole (AT) was added to SD medium to further increase stringency.

Positive interactions were assayed three times in independent replicates, while negative interactions were assayed twice.

5. SnRK1α1 immunoprecipitation and western-blotting

SnRK1α1-HA was immunoprecipitated from 5-week old rosettes of *35S::SnRK1α1-HA* plants treated for 6h in darkness, or kept in the light as controls. Wild type 5-week old rosettes of *Landsberg erecta* (*Ler*) plants were used as controls. Samples were harvested, flash-frozen and reduced to a fine powder in liquid nitrogen. Proteins were extracted with immunoprecipitation (IP) buffer [2mL buffer/g fresh weight; 50mM Tris-HCl pH 7.5, 100mM NaCl, 10mM EDTA, 0.002% (v/v) phosphatase inhibitor cocktail #2 (Sigma P572G), 0.002% (v/v) phosphatase inhibitor cocktail #3 (Sigma P0044), 0.3% (V/V) IGEPAL, 2mM DTT and 2X cOmplete™ protease inhibitor cocktail (Roche; 1 tablet/25mL)] and incubated at 4°C for 10 min. After discarding insoluble material by centrifugation, total protein concentration of the supernatant was quantified using the Bradford protein assay. For the IP, 1.2 ml of extract containing 3.5 mg protein were incubated with 40µL of anti-HA affinity matrix (Roche) with gentle rocking for 3h30min at 4ºC. Agarose beads containing immunoprecipitated proteins were recovered by a brief centrifugation at a maximum speed of 2000 rpm and washed five times with IP buffer. To elute immuno- and co-immunoprecipitated proteins, 20µL of 4X Laemmli buffer[84] were added to the beads and samples were boiled for 5 min at 95°C. For all samples, aliquots of cleared tissue lysates before the immunoprecipitation (general input) and of the supernatant after immunoprecipitation (pass-through) were kept as controls. These samples were denatured with Laemmli buffer and boiled for 5 min at 95°C, similarly to the immunoprecipitated proteins.

Proteins were resolved by SDS-PAGE, wet-transferred to a 0.45µm PVDF membrane (100 V, 70min, 4°C), and analysed by immunoblotting with anti-AGO1 (1/10000, Agrisera, AS09527) antibody, followed by an incubation with anti-HA (1/1000, Roche, #11867423001) to ensure the effectiveness of the IP.

Primary antibodies were diluted according to the manufacturers' instructions and incubated with the membrane over night at 4°C under gentle rocking. Secondary antibodies (anti-rabbit for AGO1 and anti-rat for HA) conjugated to horseradish peroxidase were diluted 1:10000 in 1% non-fat milk in TBS and incubated with the membrane for 1 h at room temperature. For detection, we used SuperSignal™

West Femto Maximum Sensitivity Substrate (Thermo Fisher). Images were acquired with a Bio-Rad ChemiDoc, using ImageLab software.

6. Phenotypical analyses

For phenotypic assays, seeds of wild type, *ago1-27*, *snrk1α1-3*, *snrk1α1-3* x *ago1-27*, SnRK1α1OE and SnRK1α1OE x *ago1-27* were sterilised and imbibed as previously described. A total of 22 seeds of each genotype were sown per plate, containing half strength Murashige and Skoog medium with 0.1% MES, 0.8% phytoagar and supplemented or not with increasing concentrations of glucose (1%, 2%, 4% or 6%), sorbitol (1%, 2%, 4% or 6%) or ABA (0.25μM, 0.5 μM, 0.75 μM or 1 μM). Plates were sealed with hypoallergenic adhesive (3M) and kept in dark at 4ºC for 2 days. After stratification the plates were incubated at 22ºC under continuous low light (70μmol m^{-2} s^{-1}) during 14 days.

Germination and cotyledon greening were scored every day except on the 6th and 13th days and all the assays were carried out in triplicate. The criterion for scoring germination was the rupture of the outer seed coat ("testa rupture"), whereas for scoring cotyledon greening the day when cotyledons greened was considered, independently of being or not expanded. Seeds that had not germinated by the end of the assay (14 days) were not scored. Germination and cotyledon greening were expressed as percentage of the total germinated seeds. Average percentages were calculated with standard error of the triplicates.

For the flowering assays, 9 seeds of each genotype were treated as previously described and after stratification were sown in soil and grown under a 16h-light (100μmol m^{-2} s^{-1}), 22ºC / 8h-dark, 18ºC regime. To quantify the flowering phenotypes, the number of rosette leaves from each individual plant was counted every two days until bolting. The number of days until bolting was also recorded. This assay was carried out in triplicate. Average numbers of days and rosette leaves to flowering were calculated for each genotype with standard error of the triplicates.

7. Introgression of the *SUC::SUL* transgene into the SnRK1 *sesquiα* mutants

SUC::SUL transgenic *Arabidopsis* plants[79] were previously crossed to SnRK1 *sesquiα2* and *sesquiα1* mutants (A. Confraria, unpublished). From the F1 progeny of these crosses, double heterozygous mutants for *snrk1α1* and *snrk1α2*, displaying the "chlorotic vein" phenotype associated with the *SUC::SUL* transgene were selected by genotyping the *snrk1α1* and *snrk1α2* mutations. Progeny of single F1 plants were sown on 0.5X Murashige and Skoog medium supplemented with 1% Sucrose and 10 ug/mL BASTA in order to select *SUC::SUL* homozygous plants. Resistant plants displaying the chlorotic vein phenotype were transferred to soil. Later, gDNA was extracted and genotyping analyses were performed for the *snrk1α1* and *snrk1α2* mutations (see below). In this way, we could ensure to recover plants of all the required *snrk1α* genotypes (*sesquiα1*, *sesquiα2*, and the corresponding single mutants). For the next round of selection, progeny of single F2 plants were sown on 0.5X Murashige and Skoog medium supplemented with 1% Sucrose and 10 ug/mL BASTA. After 10d of growth, plates with susceptible seedlings were discarded and plates with 100% resistant seedlings exhibiting the chlorotic vein phenotype characteristic of the *SUC::SUL* plants were selected. 12-18 seedlings from each plate were transferred to soil and grown in the same light conditions as before. Genotyping was performed by PCR using allele-specific primers (**Supplementary Table 1**) to select the plants with the genotypes of interest. This process was repeated until all plants bearing different SnRK1 loss-of-function mutations were homozygous for *SUC::SUL*.

8. Selection of s*esquiα*$^{SUC::SUL}$ mutants for phenotypic analyses

Given the fact that either the *snrk1α1* or the *snrk1α2* mutations are in heterozygosity in the *sesquiα* mutants and that the double *snrk1α1 snrk1α2* mutant is lethal, the progeny of *sesquiα* mutants is always a mix of seeds corresponding to the *sesquiα* itself and to a single homozygous *snrk1α* mutant. When grown under normal conditions, it is impossible to distinguish these genotypes without using an invasive genotyping-based approach. However, for being able to quantitatively and reproducibly compare *SUC::SUL* silencing in a WT vs. *sesquiα* background it would be desirable to grow plants in controlled tissue culture conditions and to avoid their wounding. I therefore set to devise a non-invasive strategy that allowed me to grow plants of all genotypes in the same conditions and at the same time be able to distinguish the *sesquiα* mutants. Work related to another project in the Baena-González lab had shown that *sesquiα* mutants display reduced hypocotyl elongation when germinated and grown for 4-5 days in darkness (M. Adamo, unpublished). Therefore, I made use of this phenotype to distinguish in a non-invasive manner *sesquiα* mutants from the single *snrk1α* mutants in the segregating *sesquiα* progeny. Sterilised and stratified seeds from previously genotyped *sesquiα*$^{SUC::SUL}$ mutants were sown on 0.5X Murashige and Skoog and grown vertically. The plate was kept under normal light (100μmol m^{-2} s^{-1}) for three hours and then covered with aluminium foil and left in the dark at 22ºC during four days. Seedlings with considerably shorter hypocotyls (corresponding to *sesquiα* mutants) were transferred to a fresh plate containing 0.5X Murashige and Skoog medium, 1% sucrose and grown horizontally under low light conditions (50 μmol m^{-2} s^{-1}) for recovery.

9. Chlorophyll extraction and quantification

Wild type and *SUC::SUL* plants (12 of each genotype) grown for 14d under low light (50 μmol m^{-2} s^{-1}) were harvested, quickly weighed, frozen with liquid nitrogen, and ground to a fine powder. Acetone [1.2 mL of 80% (V/V)] was added to each individual sample and tubes were briefly vortexed. Samples were covered with aluminium foil to prevent chlorophyll degradation and chlorophyll was extracted over night at room temperature, under rotation (40 rpm). After a centrifugation step (15 min, 4ºC, 3000 rpm), 200 μL of each supernatant were used to measure absorbance at 645 nm and 663 nm. Total chlorophyll levels were calculated as described [85] using the following equation (**Equation 1**):

Equation 1: Ca+b(mg/g) = [8.02×A663+20.20xA645]×V/1000×W (Chlorophyll a+b)

where V = volume of the extract (ml); W = Weight of fresh leaves (g).

III. RESULTS

1. Does SnRK1 affect miRNA accumulation?

To evaluate whether SnRK1 affects miRNA accumulation, SnRK1 partial loss-of-function *sesquiα2* mutants recently obtained in the Baena-González lab were used. This kind of analyses was not previously possible due to the lethality associated with complete loss of SnRK1 activity. These partial loss of function mutants have the α1-catalytic subunit knocked out and the α2-subunit knocked down [*snrk1α1*$^{-/-}$/*snrk1α2*$^{+/-}$], and despite showing significantly compromised SnRK1 signalling they are fully viable (A. Confraria, unpublished). These mutants are thereafter referred as *sesquiα2-1* or *sesquiα2-2*, depending on the *snrk1α2* allele they bear (see Materials and Methods for details).

These initial analyses were focussed on two specific miRNAs: miR156 and miR319. miR156 targets SPL transcription factors and is hence involved in the regulation of flowering time[53,86] whereas miR319 targets TCP transcription factors that are important for leaf development[54]. In addition, it was recently found that the inactivation of SnRK2 kinases, closely related to SnRK1 and core components of ABA and osmotic stress signalling pathways, leads to reduced accumulation of these specific miRNAs[87].

To see whether our SnRK1 loss of function mutants had altered accumulation of miR156 and miR319, I extracted RNA from 5-week-old rosette leaves of WT, *sesquiα2-1*, *sesquiα2-2* mutants and the corresponding parental lines and measured the levels of mature miR156 and miR319 using stem-loop quantitative RT-PCR (qPCR)[81] and specific primers (**Supplementary Table 1**).

Although not statistically significant in the case of miR156 (only two biological replicates were processed), both *sesquiα2* mutants appeared to accumulate less miR156 and miR319 (**Figure 1**) than the wild type, supporting that the partial inactivation of SnRK1 may have a negative impact in miRNA biogenesis. The single mutants, however, vary in their behaviour in what concerns the two miRNAs.

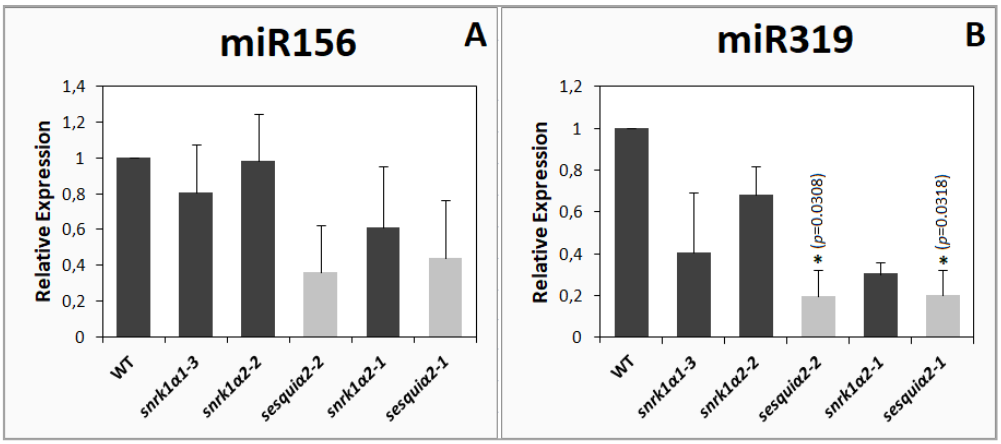

Figure 1. Relative abundance of miR156 (A) and miR319 (B) in leaves of wild type and SnRK1 loss-of-function mutants. miRNA levels were analysed by stem-loop qRT-PCR in 5-week-old rosette leaves of wild type, *snrk1α1-3*, *snrk1α2-2*, *sesquiα2-2*, *snrk1α2-1* and *sesquiα2-1*, using the geometric mean of reference genes *EIF4*, *UBQ10* and *UBC21* to normalise expression levels. Wild type was used as control sample. Bars represent SEM of two biological replicates. Asterisks indicate statistically significant differences from the wild type: * $p<0.05$ (p-value; one-way ANOVA with Dunnett's test).

2. Does SnRK1 affect miRNA activity?

Previous preliminary work in the Baena-González lab showed that, in response to stress treatments, increased SnRK1 activity and downstream miRNA-dependent gene repression was not accompanied by increased miRNA levels or increased miRNA incorporation into the silencing complex (Cláudia Martinho, PhD Thesis, UNL 2013), suggesting a potential regulation of the silencing complex itself.

Given that most miRNAs are sorted into AGO1, which ultimately conducts the cleavage or translation attenuation of complementary mRNAs, regulation of this core component of the silencing complex by SnRK1 could influence miRNA activity by driving a differential gene repression. Therefore, I decided to test the interaction between SnRK1 and AGO1 at different levels.

2.1. Physical interaction between SnRK1 and AGO1

2.1.1. Pair-wise yeast-two hybrid assays

To test the physical interaction between SnRK1 and AGO1, I started by using a yeast-two-hybrid (Y2H) pairwise assay, which is a sensitive and cost-effective means to test protein-protein interactions.

The coding sequence of *AtAGO1* was amplified from a plasmid available in the lab and the PCR product was loaded in an agarose-TAE gel. After electrophoresis, the gel showed a clear band with approximately 3150 bp, the expected size for *AGO1* coding sequence (**Figure 2.1.A**), and an unspecific PCR product. The band corresponding to *AGO1* was excised from the gel (**Figure 2.1.B**), purified and recombined into the pDONR221 vector using Gateway technology.

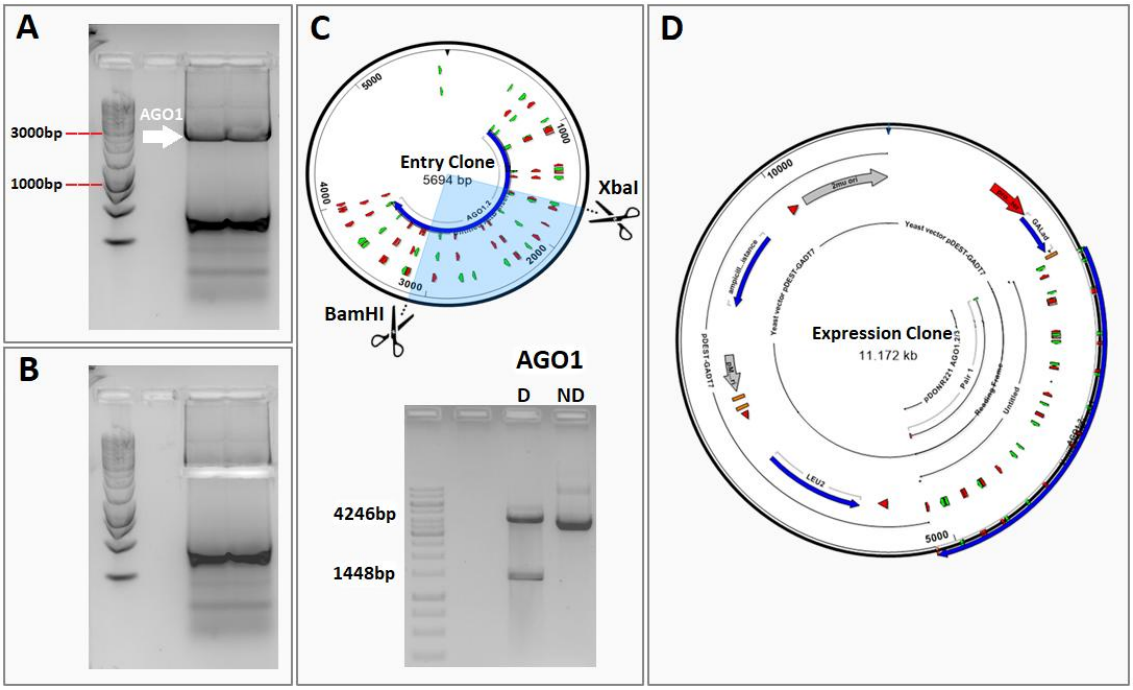

Figure 2.1. *AtAGO1* amplification and plasmid construction. A) *AGO1* was amplified from the plasmid pHBT95-*AGO1* with specific primers and **B)** the PCR product was extracted from the agarose gel to be recombined into the pDONR221 vector. **C)** Enzymatic digestion of the entry clone with two enzymes – BamHI and XbaI – revealed the expected band pattern with two bands of 4246bp and 1448bp. The sample identified as D was digested and the ND sample corresponds to the non-digested entry clone used as a control. **D)** Schematic representation of the expression clone pGADT7-AGO1.

To evaluate if the recombination was successful, the entry clone pDONR221-*AGO1* was then digested with the XbaI and BamHI restriction enzymes, having produced the expected restriction pattern. To ensure that the entry clone did not contain unexpected mutations, the full length *AGO1* insert was sequenced. Following confirmation that the sequence was correct, the entry clone was recombined by an LR reaction into the destination vector pGADT7-Dest (**Figure 2.1.D**) and the recombination sites flanking *AGO1* were sequenced to ensure that this last step yielded a functional non-mutated expression clone.

For the pairwise Y2H assay, competent yeast cells were co-transformed with pGADT7-*AGO1* and pGBKT7 constructs for expressing the various SnRK1 subunits. As controls, pGBKT7-SnRK1 subunits and pGADT7-*AGO1* were also co-transformed with the respective complementary empty vectors.

As shown in **Figure 2.2.,** cells co-transformed with *SnRK1α1* and *AGO1* grew in synthetic dropout medium lacking three amino acids (-L-H-W), whereas there was no growth in either of the controls under the same conditions, supporting that these two proteins are able to physically interact in yeast. When stringency was increased by adding aminotriazole (AT) or by removing one further amino acid (-L-W-H-A), the interaction was disrupted, indicating that the SnRK1α1-AGO1 interaction is weak.

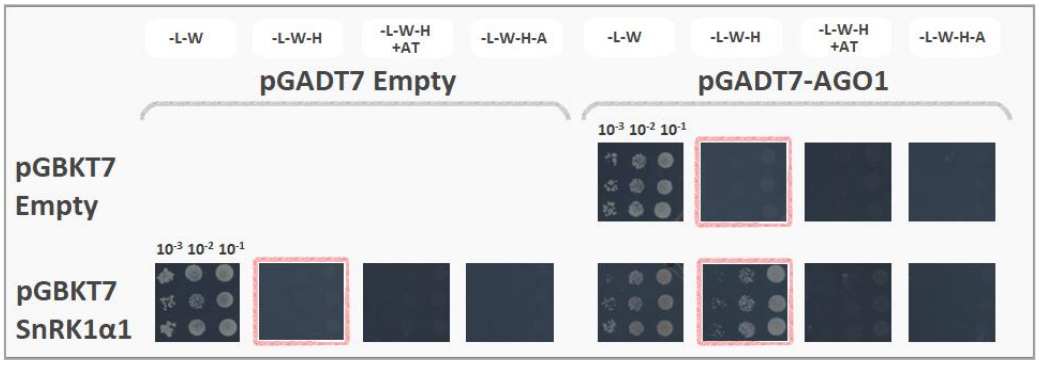

Figure 2.2. SnRK1α1 interacts with AGO1 in a pairwise yeast two hybrid assay. Ten-fold serial dilutions of saturated yeast cultures were spotted onto plates containing synthetic dropout medium with increased stringency. Growth in -L-W-H medium was observed only when cells were co-transformed with *SnRK1α1* and *AGO1*. 25 mM amino-triazole (AT) was used to increase stringency of -L-W-H medium. This assay was repeated three times with similar results. The picture shows a representative experiment.

In fact, in pairwise Y2H assays, SnRK1α1 was the only subunit for which I could detect a positive interaction with AGO1. Cells co-expressing SnRK1α2 or SnRK1β3 and AGO1 failed to grow in medium with increased stringency (**Supplementary Figure 1**). For the remaining subunits, SnRK1β1, β2 and βγ, their individual expression was sufficient to support yeast growth in -L-W-H medium, yielding a very high background growth that precluded the assessment of a possible interaction between these subunits and AGO1 (**Supplementary Figure 1**).

2.1.2. Co-immunoprecipitation

To further analyse the physical interaction between SnRK1α1 and AGO1, a co-immunoprecipitation assay was carried out using proteins extracted from rosettes of 5-week-old plants exposed to a SnRK1-activating dark treatment or kept in the light as a control. Under these conditions, we could not detect AGO1 in the fraction co-immunoprecipitating with SnRK1α1-HA either in the light or in the dark (**Figure 2.3. A** and **B**). This does not exclude that SnRK1α1 and AGO1 may still interact *in planta* in different conditions, developmental stages, or tissues.

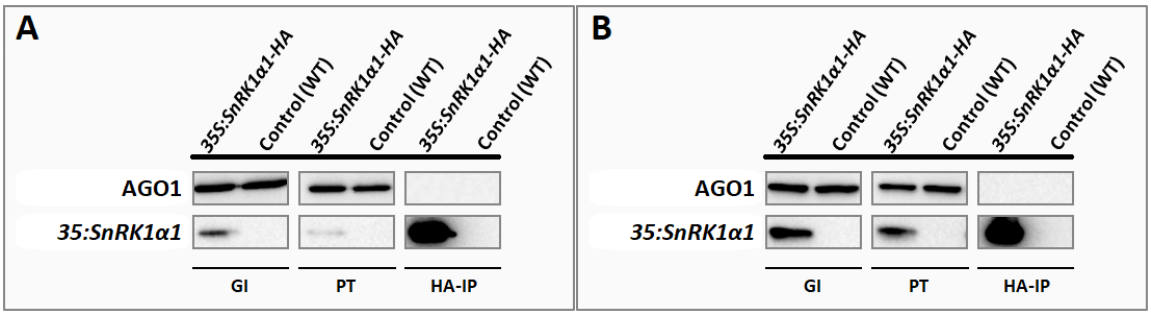

Figure 2.3. AGO1 does not co-immunoprecipitate with SnRK1α1 in mature Arabidopsis rosettes. SnRK1α1 was immunoprecipitated with high-affinity HA-agarose beads from 5-week old rosettes of *35S::SnRK1α1-HA* plants exposed to **A)** normal light conditions or exposed to **B)** a 6-hour dark treatment, using wild type as a control. Proteins co-immunoprecipitated with SnRK1α1-HA were separated by SDS-PAGE and transferred to a PVDF membrane. General input (GI), cleared tissue lysate before immunoprecipitation; Pass-through (PT), supernatant after immunoprecipitation; HA immunoprecipitate (HA-IP). AGO1 was not detected in the immunoprecitated fraction. There was no obvious difference between rosettes exposed to a SnRK1-activating dark treatment (B) and those kept in the light (A).

2.2. Genetic interaction between SnRK1 and AGO1

To further assess a potential connection between SnRK1 and AGO1, I evaluated their genetic interaction using a phenotypic characterisation of early seedling development under specific stress conditions. To this end I used *ago1-27* mutants crossed to SnRK1 loss- and gain-of-function lines. The *ago1-27* mutant bears a single nucleotide mutation in the PIWI domain that partially impairs AGO1 function[48,78]. This mutant was previously crossed to the *snrk1α1-3* knockout mutant[33] and to a SnRK1α1 overexpressor (SnRK1α1OE)[27] (N. Fernandes, unpublished). The two resulting double homozygous lines had been previously isolated.

SnRK1α1OE lines have been extensively described as hypersensitive to glucose in early seedling development[7,27,28], whereas *ago1-25* mutants were previously described as hyposensitive[88]. Glucose in high concentrations is known to induce stress responses and developmental arrest by a combination of specific glucose effects and by the consequent increase in osmotic pressure. I grew seedlings of all relevant genotypes (wild type, *ago1-27*, *snrk1α1-3*, *snrk1α1-3* x *ago1-27*, SnRK1α1OE and SnRK1α1OE x *ago1-27)* under continuous low light in 0.5X Murashige and Skoog medium supplemented with increasing concentrations of glucose, scoring germination and greening rates for 14 days. In order to distinguish between the signalling and osmotic effects of glucose, the same experiment was repeated with sorbitol as an osmolarity control.

As shown in **Figure 2.4.**, the presence of glucose in the medium delayed germination in all genotypes. As expected, SnRK1α1OE was hypersensitive, showing delayed germination in comparison to the wild type in most glucose concentrations. Interestingly, in the higher glucose concentrations (4% and 6%), SnRK1α1OE was epistatic to *ago1-27*. Under increasing sorbitol concentrations all the genotypes behaved similarly with regard to germination. Even though not statistically significant, in medium supplemented with 6% sorbitol, *ago1-27* had slightly delayed germination when compared to the wild type.

All the seeds from all the tested genotypes were able to green in plates non-supplemented with glucose/sorbitol (**Figure 2.5.A**). On the contrary, for plates supplemented with 6% glucose, all genotypes were impaired in cotyledon greening. This was not the case for medium supplemented with 6% sorbitol, showing that the glucose effects are to a large extent independent of the osmotic pressure.

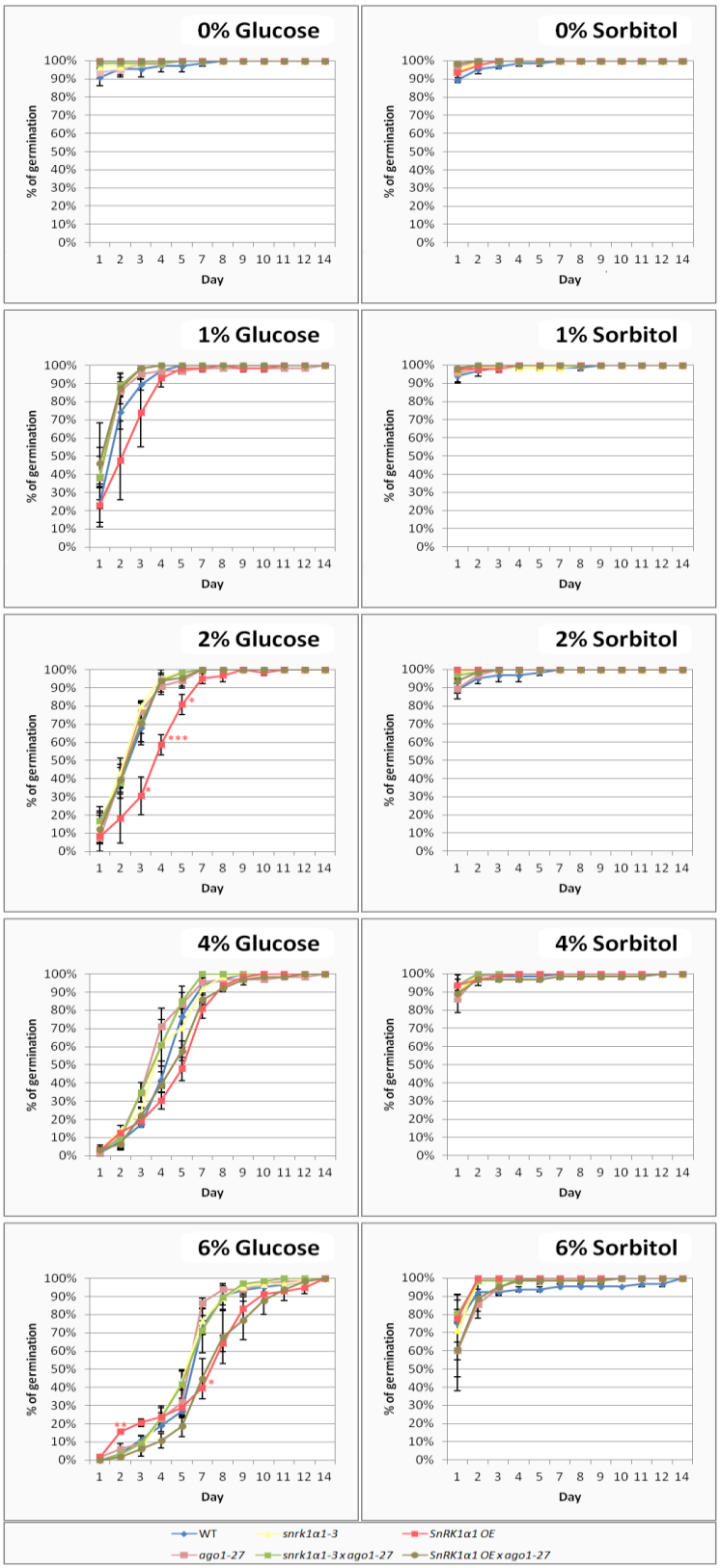

Figure 2.4. SnRK1α1 overexpressor (OE) is hypersensitive to glucose and epistatic to *ago1-27* during germination. Germination rates of wild type, *ago1-27*, *snrk1α1-3*, *snrk1α1-3* x *ago1-27*, SnRK1α1OE and SnRK1α1OE x *ago1-27* grown in 0.5X Murashige and Skoog medium supplemented with increasing concentrations (1%, 2%, 4% and 6%) of glucose (left) or of sorbitol as an osmolarity control (right). Non-supplemented control plates were included in all experiments (0% glucose/sorbitol). Seedlings were grown under continuous light (70 µmol m^{-2} s^{-1}) for 14 days, during which germination was scored daily. Values represent means ± SE from three independent experiments. Asterisks indicate statistically significant differences from the wild type: * $0.01 \leq \boldsymbol{p} < 0.05$; ** $0.001 \leq \boldsymbol{p} < 0.01$; *** $0.001 \leq \boldsymbol{p} < 0.0001$; **** $\boldsymbol{p} < 0.0001$ (*p*-value; one-way ANOVA with Dunnett's test).

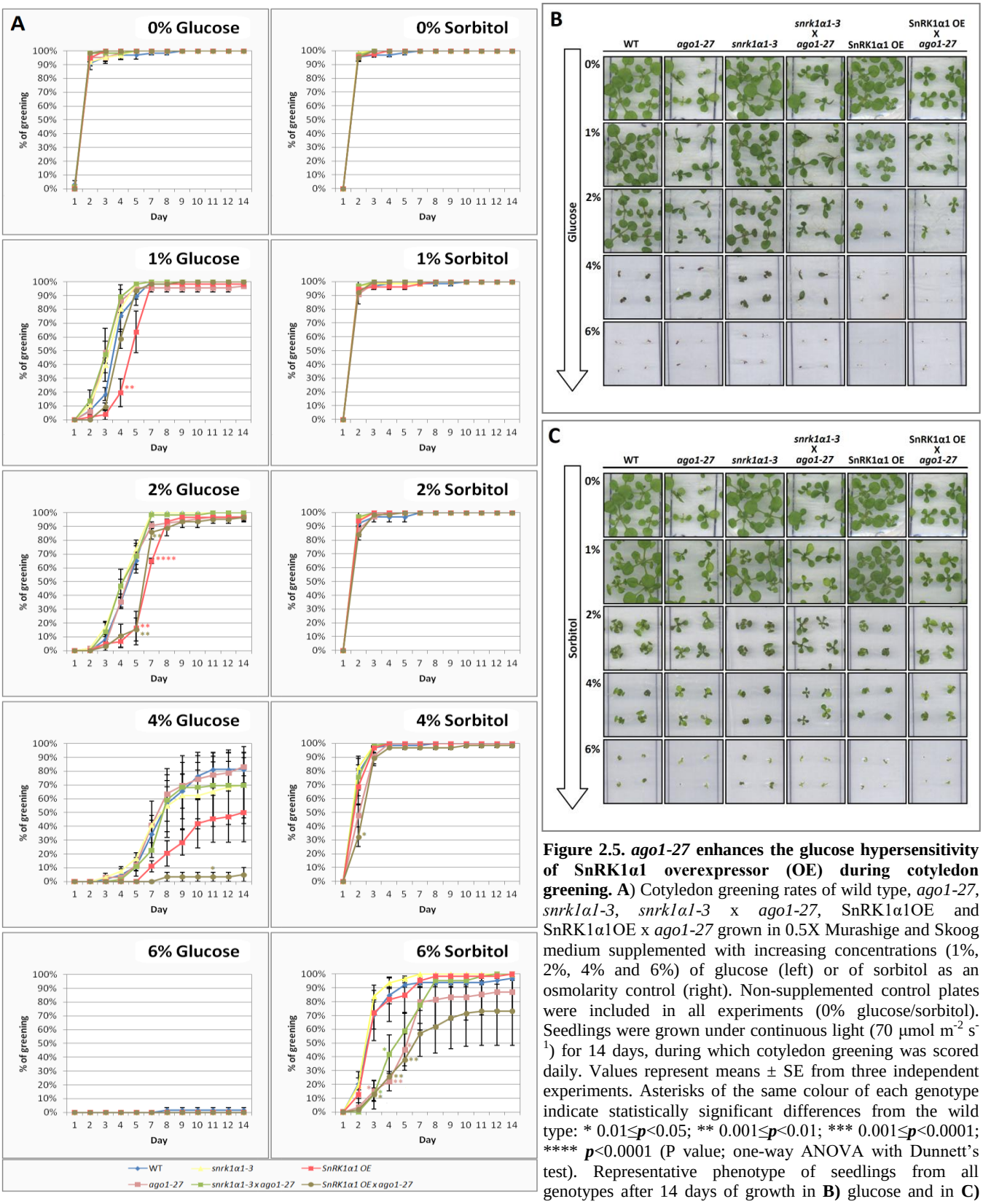

Figure 2.5. *ago1-27* enhances the glucose hypersensitivity of SnRK1α1 overexpressor (OE) during cotyledon greening. A) Cotyledon greening rates of wild type, *ago1-27*, *snrk1α1-3*, *snrk1α1-3* x *ago1-27*, SnRK1α1OE and SnRK1α1OE x *ago1-27* grown in 0.5X Murashige and Skoog medium supplemented with increasing concentrations (1%, 2%, 4% and 6%) of glucose (left) or of sorbitol as an osmolarity control (right). Non-supplemented control plates were included in all experiments (0% glucose/sorbitol). Seedlings were grown under continuous light (70 µmol m^{-2} s^{-1}) for 14 days, during which cotyledon greening was scored daily. Values represent means ± SE from three independent experiments. Asterisks of the same colour of each genotype indicate statistically significant differences from the wild type: * $0.01 \leq p < 0.05$; ** $0.001 \leq p < 0.01$; *** $0.001 \leq p < 0.0001$; **** $p < 0.0001$ (P value; one-way ANOVA with Dunnett's test). Representative phenotype of seedlings from all genotypes after 14 days of growth in **B)** glucose and in **C)** sorbitol.

Similarly to germination, and as predicted, the SnRK1α1OE seedlings were hypersensitive to glucose, displaying delayed cotyledon greening in the presence of 1%-4% glucose. On 2% glucose, SnRK1α1OE was epistatic to *ago1-27*, as in germination. Strikingly, on 4% glucose, the delay in cotyledon greening of the double mutant SnRK1α1OE x *ago1-27* was more accentuated, suggesting that *ago1-27* enhances the SnRK1α1OE delayed greening phenotype. Indeed, by day 14, SnRK1α1OE

and WT had greening rates of approximately 50% and 80%, respectively, which contrasted markedly with the 10% of the SnRK1α1OE x *ago1-27* double mutant. This effect was glucose-specific, as in the 4% sorbitol plates all seedlings from all the tested genotypes developed green cotyledons well before the 14th day.

Even though the differences were not statistically significant, the *snrk1α1-3* and the *snrk1α1-3* x *ago1-27* mutants also seemed to be slightly affected under 4% glucose when compared to the wild type. By day 14 these genotypes displayed a greening percentage of approximately 70% compared to 80% in the wild type. *ago1-27* mutants behaved similarly to the wild type in all the glucose conditions tested.

It is noteworthy that on 6% sorbitol, the *ago1-27* mutants, as well as all other genotypes harbouring the *ago1-27* mutation, displayed delayed cotyledon greening when compared to the wild type. This was particularly significant during days 3-6, but from then on there were no statistically significant differences. The most sensitive genotype appeared to be SnRK1α1OE x *ago1-27*, followed by *ago1-27*. On sorbitol, the greening rates of SnRK1α1OE were comparable to those of the wild type.

Figures 2.5.B and 2.5.C show that genotypes bearing the *ago1-27* mutation displayed similar features to the *ago1-27* parental line in terms of leaf shape and size (leaves are smaller, greener and pointy), whereas the other genotypes were comparable to the wild type. Under progressively higher concentrations of glucose/sorbitol concentrations, all plants gradually decreased in size. Whilst on sorbitol all the genotypes were similarly affected, on high glucose concentrations both SnRK1α1OE and especially SnRK1α1OE x *ago1-27* were severely impaired in cotyledon greening when compared to the remaining genotypes, in agreement with the quantification in the graphs.

In addition to glucose sensitivity, SnRK1 lines and *ago1* mutants have also been described as having altered sensitivity to ABA[27,66,89,90]. Therefore, I decided to test the early seedling development of the same genotypes on increasing ABA concentrations, in a similar experimental setup to the one used to probe glucose sensitivity.

Results show that increasing concentrations of ABA equally affected the germination rates of all the tested genotypes, except *ago1-27*, which was hypersensitive (**Figure 2.6.A**). On low concentrations of ABA, *ago1-27* was delayed in germination with major differences observed in the first counting day after stratification. After the first day these differences became progressively smaller and by the 14th day all seeds from all genotypes germinated on the ABA concentrations used. On 1μM the differences on the first day were not significant, as early germination of other genotypes was also affected.

Moreover, when analyzing the cotyledon greening rates (**Figures 2.6.B** and 2**.6.C**), I observed that all genotypes harbouring the *ago1-27* mutation were hypersensitive even in the medium supplemented with the lowest ABA concentration, whereas the SnRK1α1OE and *snrk1α1-3* parental lines behaved similarly to wild type.

For media supplemented with 0.25μM or 0.5μM ABA, SnRK1α1OE enhanced the ABA sensitivity of *ago1-27*, whereas *snrk1α1-3* partially reverted it. For ABA concentrations higher than 0.5μM all *ago1-27* genotypes were severely impaired in the greening process and indistinguishable amongst them.

Late flowering phenotypes have also been described for SnRK1α1OE lines[7,89] and *ago1* mutants[78,91]. Therefore, to further assess the genetic interaction between SnRK1 and AGO1, sterilised and stratified seeds from the same genotypes used to probe glucose and ABA sensitivity were sown in soil and grown under long day conditions. Their flowering times were subsequently quantified, counting both

the number of days ("chronological age", **Figure 2.7.A**) and of rosette leaves to flower ("developmental age", **Figure 2.7.B**).

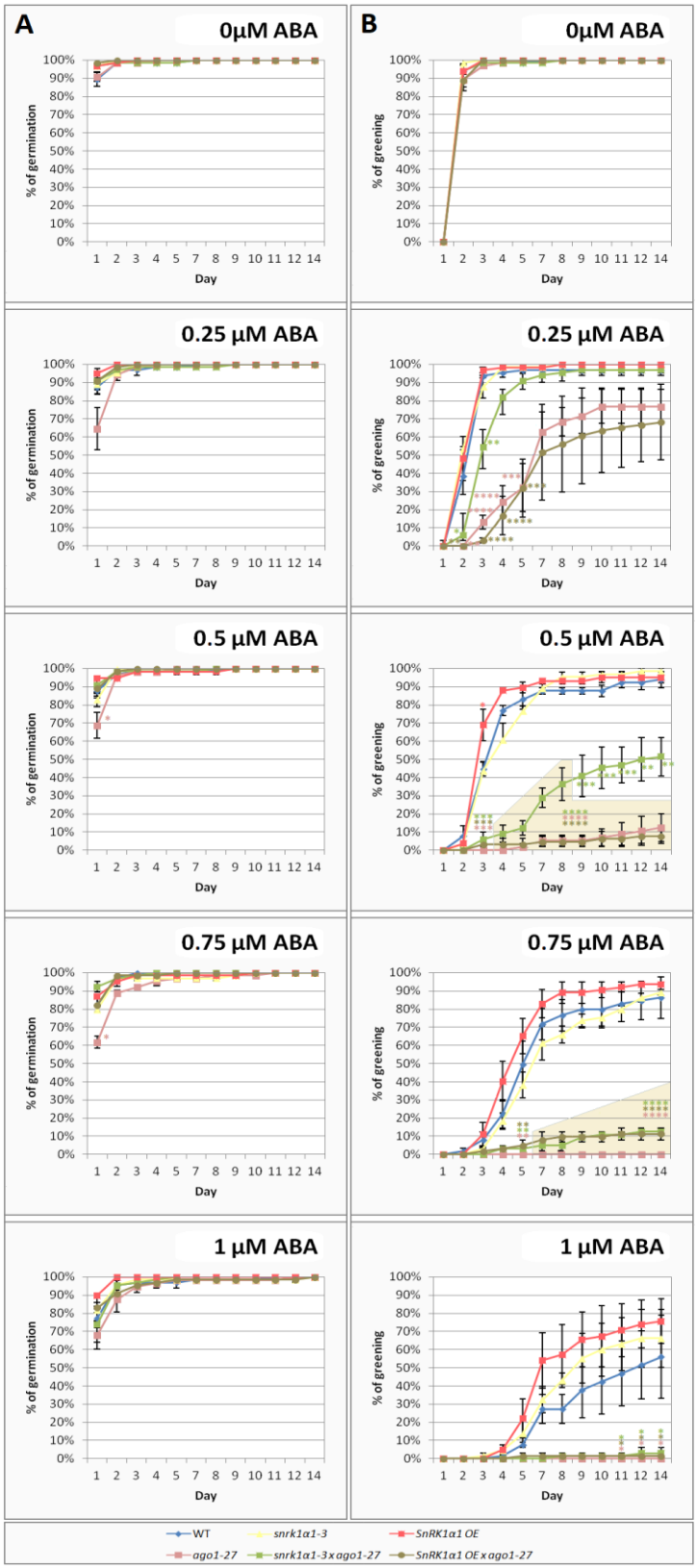

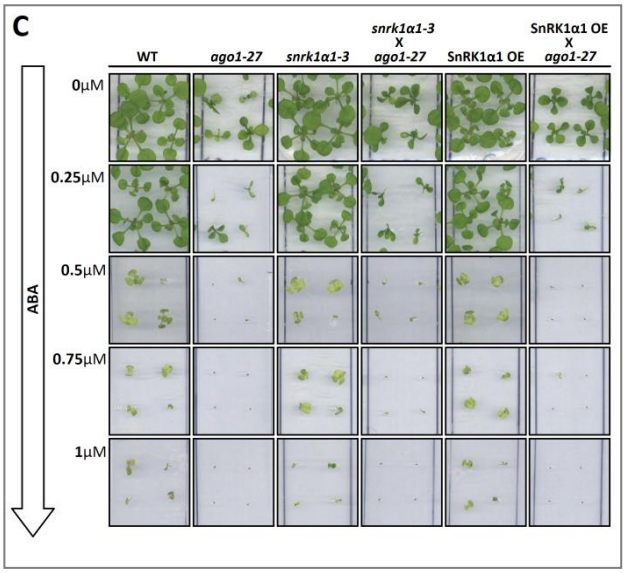

Figure 2.6. *snrk1α1-3* partially reverts the ABA hypersensitivity of *ago1-27* during germination and greening. A) Germination and **B)** greening rates of wild type, *ago1-27*, *snrk1α1*, *snrk1α1* x *ago1-27*, SnRK1α1OE and SnRK1α1OE x *ago1-27* in 0.5X Murashige and Skoog medium supplemented with increasing concentrations of ABA (0.25 µM, 0.5 µM, 0.75 µM and 1 µM) or without ABA, as a control. Seedlings were grown under continuous low light (70µmol m-2 s-1) for 14d, during which germination and greening were scored daily. Values represent means ± SE from three independent experiments. Asterisks of the same colour of each genotype indicate statistically significant differences from the wild type: * $0.01 \leq p < 0.05$; ** $0.001 \leq p < 0.01$; *** $0.001 \leq p < 0.0001$; **** $p < 0.0001$; dots confined to the darker area of the graph correspond to a $p < 0.0001$ (P value; one-way ANOVA with Dunnett's test). **C)** Representative phenotype of seedlings from all genotypes after 14 days of growth in ABA.

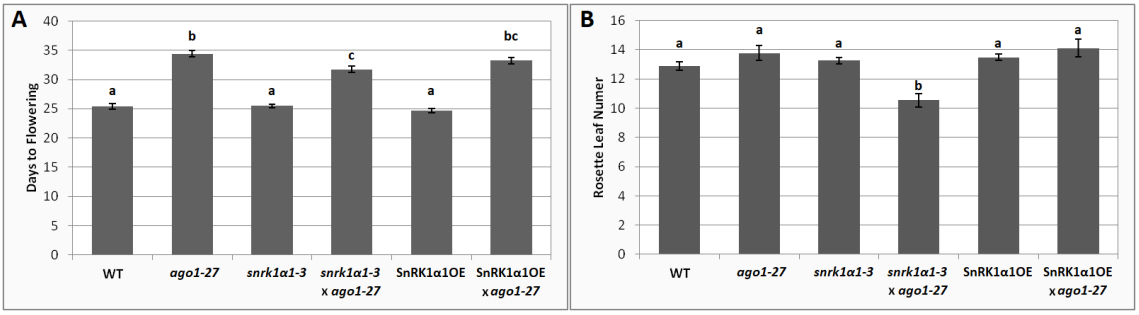

Figure 2.7. *snrk1α1-3* partially reverts the delayed flowering of *ago1-27* mutants. A) Days to flowering and **B)** number of rosette leaves of wild type, *ago1-27*, *snrk1α1-3*, *snrk1α1-3* x *ago1-27*, SnRK1α1OE and SnRK1α1OE x *ago1-27* grown under long day conditions (16h light/8h dark; 100 µmol m^{-2} s^{-1}). Values represent means ± SE of three independent replicates. Different letters indicate statistically significant differences ($p < 0.05$; ANOVA with Tukey's test).

Results showed that overall *ago1-27* mutants displayed a delayed flowering phenotype when grown in long days, flowering later and producing more rosette leaves than the wild type, in accordance to what has been described in the literature. Interestingly, *snrk1α1-3* partially reverted the delayed flowering phenotype of *ago1-27* mutants, with the double mutant flowering approximately 3 days earlier than *ago1-27* (**Figure 2.7.A**) and having on average 2 leaves less than the wild type by the time it flowers (**Figure 2.7.B**).

The *snrk1α1-3* mutant behaved similarly to the wild type for both tested criteria and so did SnRK1α1OE, contrary to what was previously described. Although the number of rosette leaves of the SnRK1α1OE was slightly higher when compared to the wild type, the difference was not statistically significant.

2.3. Functional interaction between SnRK1 and AGO1

In parallel with approaches described above to tackle the putative interaction between SnRK1 and AGO1, an experimental setup was conceived to test whether SnRK1 is able to functionally interact with AGO1 using the *SUC::SUL* silencing reporter system[79,80].

In this silencing reporter system, a dsRNA of the *SULPHUR* gene (*SUL*) is expressed under control of the *SUC2* promoter (**Figure 2.8.**), which is specific for phloem companion cells[92]. *SUC::SUL* transgenic *Arabidopsis* plants consequently produce a *SUL* hairpin structure that is recognised and processed by DICER proteins leading to the formation of short interfering RNAs (siRNAs) and the silencing of the endogenous *SUL* mRNA. The repression of this transcript leads to reduced levels of the Mg^{2+}chelatase, an enzyme essential for the biosynthesis of chlorophyll, therefore resulting in the chlorosis of the silenced cells in the vasculature (**Figure 2.8**).

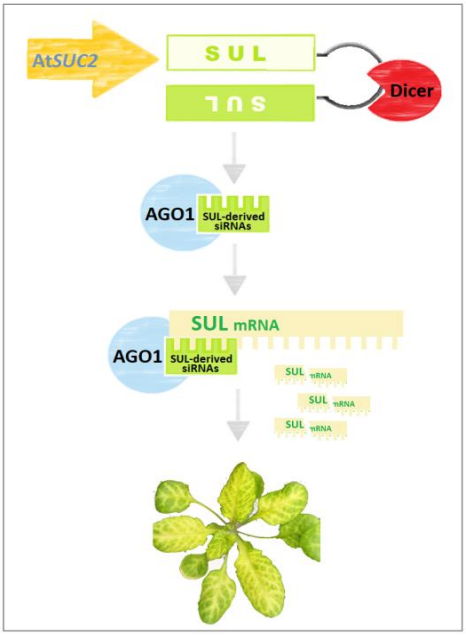

Figure 2.8. *SUC::SUL* silencing reporter system. The AtSUC2::senseSUL-antisenseSUL construct is processed by Dicer-like proteins and SUL-derived siRNAs are loaded into AGO1 to silence the endogenous *SUL* transcript, promoting the chlorosis of the phloem companion cells.

To test the functional interaction between SnRK1 and AGO1, *SUC::SUL* transgenic *Arabidopsis* plants[79] were previously crossed to SnRK1 partial loss-of-function mutants (*sesquiα2-1* and *sesquiα2-2*) (**Figure 2.9**). From the F1 progeny of these crosses, double heterozygous mutants for *snrk1α1* and *snrk1α2*, displaying the "chlorotic vein" phenotype, were selected by genotyping *snrk1α1* and *snrk1α2*. Progeny of single F1 plants were sown on 0.5X Murashige and Skoog medium supplemented with 1% sucrose and 10 µg/mL BASTA. Resistant plants displaying the chlorotic vein phenotype were transferred to soil. Later, gDNA was extracted to genotype for the *snrk1α1* and *snrk1α2* mutations. In this way, plants of all the required genotypes, with the exception of *sesquiα2-1* and *sesquiα1-2*, carrying the *SUC::SUL* insertion were successfully isolated. This included WT, *snrk1α1-3*, *snrk1α2-1*, *snrk1α2-2*, *sesquiα2-2* (*snrk1α*$^{-/-}$/*snrk1α2-2*$^{+/-}$) and *sesquiα1-1* (*snrk1α*$^{+/-}$/*snrk1α2-1*$^{-/-}$) (**Figure 2.10.A**). Progeny of single F2 plants were sown again on 0.5X Murashige and Skoog medium supplemented with 1% sucrose and 10 µg/mL BASTA to select combinations of 100% *SUC::SUL* phenotype. For the cases in which this was not possible in this generation, the selection process was carried for one further generation to obtain homozygous *SUC::SUL* in all the different backgrounds.

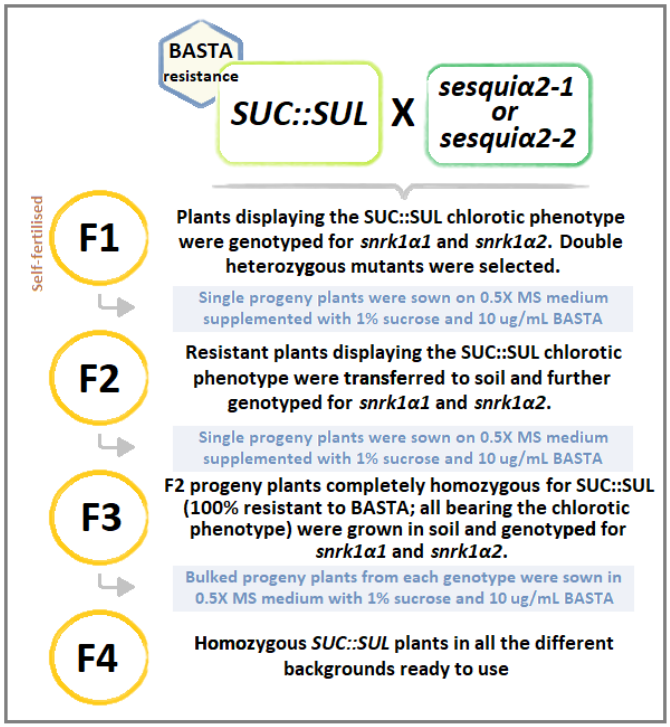

Figure 2.9. Schematic representation of the selection process of SnRK1 loss-of-function mutants homozygous for *SUC::SUL*. Steps employed in the selection process of homozygous *SUC::SUL* plants in different SnRK1 loss-of-function backgrounds.

Considering that siRNAs are, likewise miRNAs, loaded into AGO1[93], the following step of this strategy was to grow plants from each genotype in the same conditions and assess the functional interaction between SnRK1 and AGO1 by measuring total chlorophyll and *SUL* transcript levels.

However, given that the progeny of the *sesquiα* plants is heterogenous, containing in addition to the *sesquiα* itself the corresponding single homozygote mutant, I had to devise a non invasive strategy to distinguish these two co-segregating genotypes.

Dark-grown *Arabidopsis* seedlings grow elongated, etiolated hypocotyls[94,95]. Moreover, unpublished work from the Baena-González group showed that dark-grown *sesquiα* seedlings have considerably shorter hypocotyls than its parental lines and WT grown in the same conditions. Therefore, seeds from all genotypes were sterilised and sown on vertically displayed plates containing 0.5X Murashige and Skoog medium. After three hours under normal light conditions (100 µmol m^{-2} s^{-1}) I covered the plates, keeping them in the dark for 4 days. During this time, all genotypes developed etiolated hypocotyls longer than the *sesquiα* mutants, enabling me to distinguish them from the other seedlings (data not shown). Moreover, to confirm if the seedlings with shorter hypocotyls were indeed *sesquiα*, a genotyping-based approach was carried out further reinforcing that this selection method is reliable (data not shown).

Seedlings from all genotypes were thereafter transferred to plates with 0.5X Murashige and Skoog medium supplemented with 1% sucrose and grown horizontally under low light conditions (50 µmol m^{-2} s^{-1}) for 14 days, after which plants would have been harvested and total chlorophyll and *SUL* transcript levels would have been measured.

Due to time constraints, contamination problems and the low abundance of *sesquiα* seeds I could not obtain results with this system, but nonetheless a method to measure total chlorophyll levels was tested and can be used in the future in this setup. WT and *SUC::SUL* seeds were treated as described above and by the end of day 14, 12 plants from each genotype (**Figure 2.10.B**) were harvested and used for chlorophyll quantification. Results showed that the WT plants had on average three times more total chlorophyll than the WT *SUC::SUL* plants (**Figure 2.10.C**).

This approach alongside with specific quantitative RT-PCR primers for the *SUL* transcript will represent powerful tools to assess the functional interaction between SnRK1 and AGO1 in a near future.

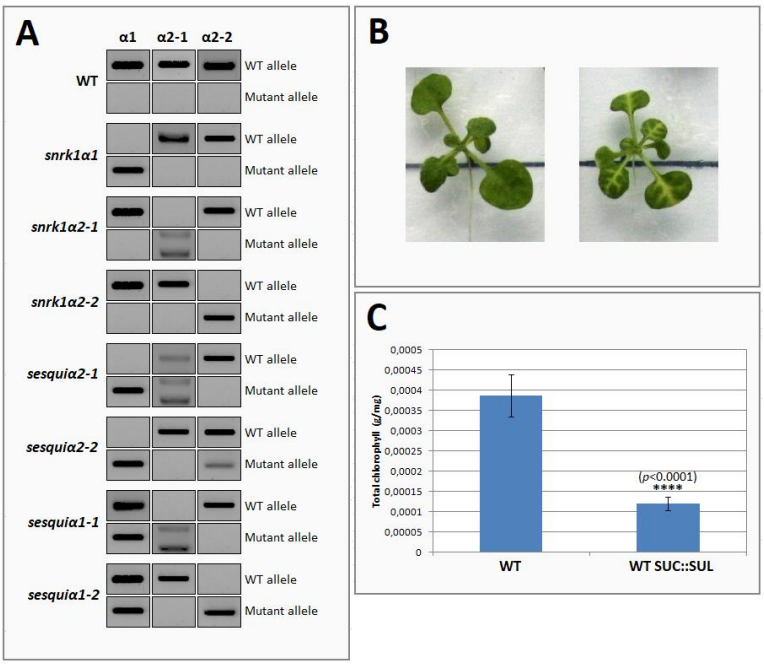

Figure 2.10. Strategy steps to assess the functional interaction between SnRK1 and AGO1. A) PCR-based genotyping of wild type *SUC::SUL* plants and *SUC::SUL* lines containing SnRK1 mutations: *snrk1α1-3*, *snrk1α2-1*, *snrk1α2-2*, *sesquiα2-1*, *sesquiα2-2*, *sesquiα1-1* and *sesquiα1-2*. **B)** Representative phenotype of seedlings from wild type (left) and *SUC::SUL* (right) genotypes after 14 days of growth under low light conditions (50 µmol m^{-2} s^{-1}). **C)** Total chlorophyll levels of WT and *SUC::SUL* plants were measured through absorbance readings and calculated using the equation: Ca+b(mg/g) = [8.02×A663+20.20xA645]×V/1000×W (Chlorophyll a+b) where V = volume of the extract (ml); W = Weight of fresh leaves (g); Bars represent means ± SE of 12 plants per genotype.

IV. DISCUSSION

SnRK1 functions as an energy sensor, being repressed in sugar-replete conditions and activated when energy levels decline for example as a consequence of stress. Upon activation, SnRK1 triggers metabolic readjustments through direct enzyme phosphorylation, and a massive transcriptomic reprogramming to restrict energy consumption and maximise energy production, altogether promoting homeostasis and plant survival[9]. Regarding the transcriptional effects of SnRK1, bZIP transcription factors are well-established downstream effectors of the SnRK1 signalling cascade, inducing the expression of target genes largely related to amino acid metabolism[96]. Gene repression, on the other hand, is less understood but appears to partly rely on miRNA activity[36]. However, how SnRK1 affects the miRNA pathway is unknown. miRNAs are small RNAs that control gene expression mainly through cleavage or translational repression of complementary target mRNAs. In plants, environmental stimuli and internal cues regulate the accumulation of specific miRNAs[97] that have been extensively implicated in developmental processes as well as in responses to different types of stress[57].

To better understand the connection between SnRK1 and miRNAs two non-mutually exclusive hypotheses were proposed in this thesis: a) SnRK1 affects miRNA biogenesis and b) SnRK1 influences miRNA activity.

To test the first hypothesis, I compared the accumulation of two specific miRNAs, miR156 and miR319, in wild type plants and SnRK1 knockdown mutants (*sesquiα* mutants), uncovering a deficiency in the accumulation of these miRNAs when SnRK1 function is compromised (**Figure 1**). If this deficiency is confirmed in future studies, it could support the hypothesis that SnRK1 affects miRNA biogenesis, since defects in miRNA biogenesis often lead to altered levels of mature miRNAs[37]. However, accumulation of mature miRNAs within tissues is also influenced by other factors such as miRNA stability and turnover. To demonstrate that SnRK1 influences indeed miRNA biogenesis, it would be important to quantify the levels of primary miRNAs (pri-miRNAs). Mutations affecting central components of the miRNA biogenesis machinery are often associated to higher levels of pri-miRNAs and, due to deficient processing, lower levels of the corresponding mature miRNAs[98]. Accordingly, if SnRK1 affects miRNA biogenesis by interacting with one of these components, a decrease in SnRK1 activity, as in the *sesquiα* mutants, should result in increased levels of pri-miRNAs. Interestingly, recent findings showed that mutants impaired in the related SnRK2 kinases accumulated higher levels of specific pri-miRNAs and lower levels of mature miRNAs, including miR156, miR160, and miR319. This was suggested to result from the reported interaction between SnRK2 kinases and components of the miRNA biogenesis machinery such as SERRATE (SE) and HYL1[87]. Moreover, independent phosphoproteomic studies unveiled SE as a potential target for SnRK1 under energy deprivation[30]. If this is confirmed, SE could be a common target of SnRK1 and SnRK2 kinases. It would be interesting in the future to investigate this putative interaction between SnRK1 and SE using Y2H and co-immunoprecipitation approaches, and complement this with *in vitro* kinase assays and mass spectrometry to confidently identify the residues phosphorylated by SnRK1 in SE. Upon identification of these phosphoresidues, it would also be important to test their functional relevance *in vivo*, for example using the corresponding SE phosphomutant versions to complement the *se* mutant.

It is also not clear at this point whether the observed decrease in miR156 and miR319 levels is general or specific. To clarify this issue, it would be necessary to quantify the levels of other miRNAs in the *sesquiα* mutants. In any case, it is also plausible that the SnRK1 effect is specific to these two miRNAs or a miRNA subset. The switch from the juvenile-to-adult phase is partially controlled by

miR156 and its targets, the SPL transcription factors. Over the course of development the abundance of miR156 decreases and the *SPL* transcript levels increase in a coordinated manner to induce floral transition[99]. Interestingly, miR156 abundance increases and flowering time is delayed in *Arabidopsis* plants grown under various stress conditions, such as high salinity and drought[100]. Conversely, sugars have been shown to repress miR156 expression at both the transcriptional and post-transcriptional levels[101,102]. On the other hand, SnRK1 is activated under stress situations and inhibited by sugars[8] and *sesquiα* mutants accumulating less miR156 display an early flowering phenotype (unpublished work from the Baena-González lab). Based on these observations, it is tempting to speculate that SnRK1 may regulate miR156 abundance.

On the other hand, miR319 is known to target TCP transcription factors, implicated in the regulation of plant architecture[103], leaf development[104,105], hormone pathways[106–108], and responses to biotic and abiotic stress, such as salinity and drought[109–111]. Additionally, two transcripts targeted by miR319, *TCP4* and *TCP2*, decreased in response to transient SnRK1 activation by darkness in a miRNA-dependent manner[36], which is in line with the lower accumulation of this miRNA in the *sesquiα* mutants. SnRK1 may be influencing miR319 levels to regulate mitochondrial energy metabolism, as TCPs have also been shown to regulate nuclear-encoded mitochondrial genes[112].

Previous results from the Baena-González Group showed that repression of some transcripts, including *TCP2*, *TCP4* and a *PPR*, upon transient SnRK1 activation was dependent on miRNAs[36] (Cláudia Martinho, PhD Thesis, UNL 2013). Nevertheless, at least in the case of the *PPR* transcript, its down regulation was not due to differences in miRNA accumulation or miRNA loading into the RISC complex (Cláudia Martinho, PhD Thesis, UNL 2013), which prompted the hypothesis that SnRK1 could modulate miRNA activity by modifying some component of the RISC complex. miRNA activity can be regulated through AGO1 independently of miRNA accumulation. Supporting this are the slicing- defective *ago1* mutants that, despite accumulating nearly normal levels of miRNAs, show defects in target mRNA repression[113]. Additionally, a few AGO1 interactors were shown to impact on its activity, without interfering with miRNA or AGO1 levels; these include SQUINT, which facilitates RISC assembly[114], and EMA1 and TRANSPORTIN1, two importin β proteins that negatively and positively regulate miRNA activity, respectively[115,116]. Moreover, AGO1 abundance has been shown to be regulated by autophagy[117], which is a process positively regulated by SnRK1[118].

Posttranslational modifications of human AGO2 (the most similar ARGONAUTE protein to plant AGO1), such as hydroxylation and phosphorylation, have been also described[119,120]. While hydroxylation was shown to influence AGO2 stability and subcellular localisation[119], phosphorylation was shown to affect small RNA binding[121], miRNA maturation in response to hypoxia[122] and miRNA-mediated silencing[123–125]. Previous bioinformatics analyses predicted eight putative SnRK1 phosphorylation residues in AGO1, suggesting that SnRK1 could phosphorylate AGO1 and modulate its function (Cláudia Martinho, PhD Thesis, UNL 2013). Altogether, this led me to select the major slicing effector AGO1 as the main candidate to test whether SnRK1 could affect miRNA activity.

I started by investigating the physical interaction between SnRK1 and AGO1 in an Y2H assay. While cells co-expressing SnRK1α2 or SnRK1β3 with AGO1 failed to grow in selective medium (**Supplementary Figure 1**), yeast cells co-transformed with SnRK1α1 and AGO1 were clearly able to grow in synthetic dropout medium lacking three amino acids (-L-H-W), thus unveiling an interaction between the two proteins in yeast (**Figure 2.2**). For the remaining subunits, β1, β2 and βγ, it was not clear if they interacted with AGO1 because their individual expression yielded a very high background growth (**Supplementary Figure 1**).

However, the physical interaction between SnRK1α1 and AGO1 could not be confirmed *in planta*. Using protein extracts of 5-week-old rosettes kept in the light as a control or exposed to a SnRK1-activating dark treatment, I could not co-immunoprecipitate AGO1 with SnRK1α1-HA (**Figure 2.3. A** and **B**). Despite the apparent conflict with our Y2H results, it must be noted that a positive result in an Y2H system does not necessarily imply an interaction *in planta*, and on the other hand a negative result in a co-immunoprecipitation assay does not preclude the existence of an actual interaction. Therefore, based on these results, several scenarios can be considered. It is possible that the interaction is transient or weak, making it difficult to detect and potentially requiring the use of cross-linkers to be preserved. It is also possible that the interaction is not stable because of the extraction and incubation conditions employed, and in this case the concentration of detergent and/or salt could be adjusted. Moreover, the interaction may only occur in specific tissues or developmental stages or even upon other stress conditions. Indeed, AGO1 expression levels are clearly higher in inflorescences comparatively to green tissues[126] and *ago1* hypomorphic mutants are hypersensitive to ABA during early seedling development[66,88], and therefore it would be important in the future to replicate this assay using other tissues where AGO1 is more expressed and other stress treatments such as ABA. It is also plausible that, despite the interaction in yeast, AGO1 and SnRK1α1 do not interact *in planta*.

To further assess a potential connection between SnRK1 and AGO1, *ago1-27* mutants were crossed to SnRK1α1 loss- and gain-of-function mutants and their genetic interaction was evaluated using a phenotypic characterisation of early seedling development where germination and cotyledon greening rates were analysed under increasingly high concentrations of glucose or ABA (summarised in **Table 1**). In Arabidopsis, SnRK1α1 overexpressors are hypersensitive to glucose during early seedling development[7,27,28], whereas *ago1-25* mutants were described as glucose hyposensitive[88]. Given this, as well as the previous findings that SnRK1 induces target gene repression via miRNAs[36] one could expect that under high glucose concentrations (stressful condition), SnRK1 would repress growth at least partly through the stimulation of AGO1 activity. In this case the expectation is that the *ago1-27* mutation would partially revert the hypersensitive phenotype of SnRK1α1OE. In addition, if glucose sensitivity requires SnRK1, *snrk1α1*-3 should be more insensitive to glucose than the wild-type in these conditions. However, even though our results confirmed previous findings that the SnRK1α1OE is hypersensitive to glucose both during germination and greening[27,28] (**Figures 2.4** and **2.5.A**), *snrk1α1-3* was not insensitive, indicating that even though SnRK1 enhances sugar sensitivity, the lack of SnRK1α1 is not sufficient to impair glucose responses. Moreover, *ago1-27*, unlike *ago1-25*, was not hyposensitive to glucose, and behaved much like the WT (**Figures 2.4** and **2.5.A**), suggesting that even though they are both hypomorphic alleles and result from a single point mutation in the PIWI domain (G758S in the case of *ago1-25* and A992V in the case of *ago1-27*)[78], they possibly affect different aspects of AGO1 function. Also contrary to my expectations, SnRK1α1OE was epistatic to *ago1-27* in 6% glucose with regard to germination (**Figure 2.4**), and surprisingly the glucose sensitivity of SnRK1α1OE during greening in 4% glucose was clearly enhanced by the *ago1-27* mutation (**Figure 2.5.A**). It should be noted though that exposure to sorbitol did not reproduce the effects of high concentrations of glucose (**Figure 2.5.A**), indicating that the glucose-mediated delay of seedling development was not due only to osmotic stress. However, it is not totally clear why *ago1-27* enhances the SnRK1α1OE hypersensitivity to glucose while the *ago1-27* mutant alone behaves like the WT under the same conditions. Although the glucose hypersensitivity could partly be due to an increase in ABA levels caused by the exposure to high sugars (**Figure 3.1.**), one would expect in this case some degree of glucose hypersensitivity in the single *ago1-27*.mutant. Instead, the fact that the *ago1-27* mutation is sensitised in the SnRK1α1OE background may suggest that part of the SnRK1 effects in high glucose stress are mediated by AGO1 repression.

Table 1.1. Summarised phenotypic characterization of germination and cotyledon greening under high concentrations of glucose or ABA. Comparative table of different degrees of sensitivity to high concentrations of glucose (green) or ABA (red) during germination and cotyledon greening between wild type plants and *ago1-27*, *snrk1α1-3*, *snrk1α1-3* x *ago1-27*, SnRK1α1 OE and SnRK1α1 OE x *ago1-27* mutants. The minus symbol represents phenotypes similar to the WT; the plus symbol stands for increased sensitivity; the number of plus symbols directly correlates to the degree of hypersensitivity.

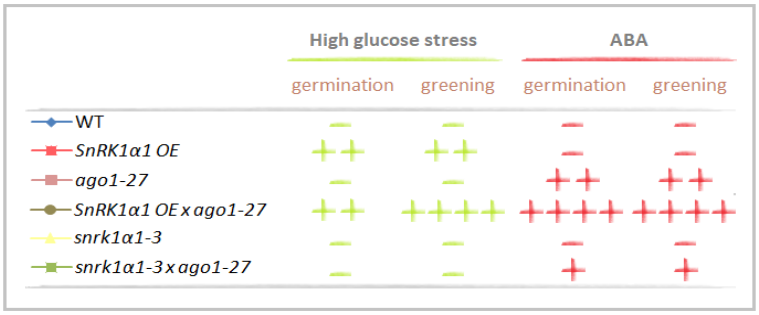

On the other hand, it was previously reported that both SnRK1α1OE[27] and *ago1* hypomorphic mutants[66,90] are hypersensitive to ABA. ABA was previously shown to activate SnRK1 through repression of PP2C phosphatases[28]. Furthermore, SnRK1 phosphorylates and positively regulates FUS3, a transcription factor that promotes seed dormancy by repressing gibberellic acid (GA) biosynthesis (the main phytohormone responsible for germination) and by promoting ABA synthesis[89,127–129]. Additionally, SnRK1 was also shown to phosphorylate *in vitro* ABI5[130], a major transcription factor of the ABA pathway that induces a developmental arrest during early seedling growth in response to ABA[131]. Altogether, these findings could explain, at least in part, the hypersensitive behaviour of the SnRK1OE, in which the overactivation of SnRK1 would enhance the mechanisms described above. Consistently, under the hypothesis that AGO1 is downstream of SnRK1, the hypersensitivity of both SnRK1α1OE and *ago1* to ABA can only be explained if SnRK1 has a repressive effect on AGO1. The results presented in this work showed that under ABA treatment, *ago1-27* was delayed in germination (**Figure 2.6.A**) and severely affected in greening (**Figure 2.6.B**). The double mutant SnRK1α1OE x *ago1-27* displayed enhanced hypersensitivity to ABA (**Figure 2.6.B**), but in contrast to previous reports[27], I was not able to observe ABA hypersensitivity in the SnRK1α1OE. The reason behind this apparent conflict may be the ABA concentration used in the previous work and mine (2.5 μM ABA and 1 μM ABA, respectively). Additionally, other factors such as light conditions and the age of the seeds could also influence the response to ABA. Light intensity is directly related to endogenous sugars[132] whose accumulation influences ABA levels and older seeds require more ABA to promote growth arrest. In my assays I used lower light conditions (70 μmol m^{-2} s^{-1}) than those normally used (100 μmol m^{-2} s^{-1}) and the SnRK1α1OE seeds used were slightly older than those of the WT, which could also explain why SnRK1α1OE was not hypersensitive to ABA in these experiments. Regarding *snrk1α1-3*, one could expect ABA hyposensitivity, a phenotype opposite to that of SnRK1α1OE. Although my results showed that *snrk1α1-3* was not hyposensitive to ABA and behaved similarly to the WT (**Figures 2.6.A** and **B**), probably due to redundancy of the SnRK1α2 catalytic subunit, the double mutant *snrk1α1-3 x ago1-27* indeed was less sensitive than *ago1-27* at least for ABA concentrations until 0.5 μM (**Figure 2.6.B**).

Taken together, these results do not support a model in which SnRK1 acts through AGO1 to repress early seedling development, as I initially predicted. On the contrary, SnRK1 may repress AGO1 function and in turn AGO1 may be a negative regulator of SnRK1 or function in a parallel pathway to promote early seedling development (**Figure 3.1.**). However, one must bear in mind that the mechanisms operating during the short-term activation of SnRK1[36] may be different from those of the long-term manipulation of SnRK1 (this thesis). It is plausible that upon sudden and extreme stress treatments, SnRK1 activation indeed results in AGO1 phosphorylation and increased capacity to

repress gene expression, whereas other levels of regulation come into play when SnRK1 is constitutively manipulated in plants, causing the opposite effect. In fact, Li et al.[66] have shown that under ABA and abiotic stress treatments miR168 expression is induced to repress the *AGO1* transcript and thereby maintain AGO1 homeostasis. Moreover, and in line with our results, it was also reported that AGO1 is a negative modulator of ABA signalling and stress responses in Arabidopsis[66]. It is therefore tempting to suggest that under the long-term activation of SnRK1 a similar regulatory mechanism could take place.

Interestingly, further support of AGO1 being a negative regulator of SnRK1 comes from the flowering

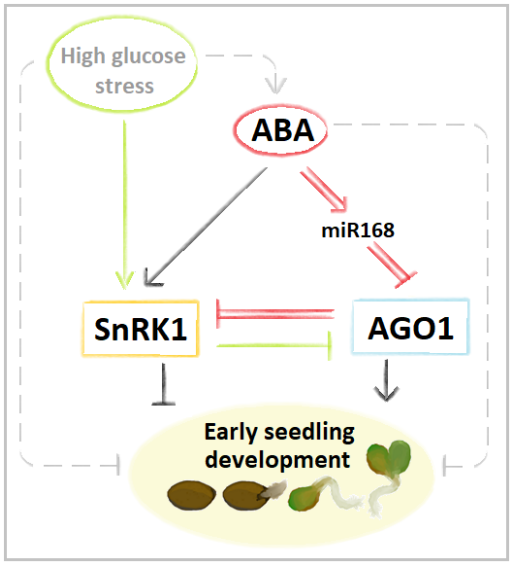

Figure 3.1. Schematic representation of the possible mode of action of SnRK1 and AGO1 during germination/early seedling development under high glucose stress or ABA. SnRK1 and AGO1 negatively regulate each other in both stress conditions. Under high glucose stress the SnRK1 pathway predominates and the AGO1 contribution is visible only when SnRK1 is activated (green lines). Under ABA, the repression of AGO1 predominates and the SnRK1 contribution is visible only when AGO1 function is compromised in the *ago1-27* mutant (red lines); grey dashed lines represent unknown mechanisms.

phenotype of the double mutant *snrk1α1-3 x ago1-27* (**Figure 2.7.A** and **B**; summarised in **Table 2**). Even though in the tested conditions the difference in flowering time between the mutant and wildtype plants was not significant (**Figure 2.7.A** and **B**; summarised in **Table 2**), SnRK1OE has been described as late flowering. In contrast, unpublished results in the Baena-González lab showed that *sesquiα* mutants are early flowering. However, due to the redundancy between the *α*-subunits, the flowering phenotype of *snrk1α1-3* is similar to that of the wild type[7,89]. *ago1-27* mutants, on the other hand, have been previously described as late flowering[91], which was also observed in this experiment (**Figure 2.7.A** and **B**; summarised in **Table 2**). Albeit carrying approximately normal levels of AGO1, *ago1-27* mutants are impaired to a great extent in posttranscriptional gene silencing, which may explain, at least partially, their delayed flowering phenotype. Several pathways integrate environmental and internal cues to regulate the flowering time[53]. The age pathway is mainly controlled by two miRNAs, miR156 and miR172, that have opposite effects in the control of flowering time. Over the course of plant development, a decrease in miR156 and *AP2-like* transcripts (miR172 targets and flowering repressors) is accompanied by an increase in the expression of miR172 and *SPL* mRNAs (miR156 targets and flowering promoters) (**Figure 3.2.A**), thus promoting flowering[45,99,133,134]. However, although some cases of cleavage-mediated silencing of miR172 targets have been previously reported[45,133,135–137], the flowering repressors *AP2-like* genes are mainly inhibited through translation repression[45,46]. In a scenario where AGO1 is clearly affected in translation repression, such as in the case of *ago1-27* mutants[48], it is plausible that the repression of *AP2*-like

genes is compromised (**Figure 3.2.B**) thereafter delaying the flowering onset. Curiously, the double mutant *snrk1α1-3 x ago1-27* flowered in average two days earlier than *ago1-27* (**Figure 2.7.A**; summarised in **Table 2**) and did so even with less rosette leaves than the wild type (**Figure 2.7.B**; summarised in **Table 2**), therefore partially reverting the *ago1-27* late flowering phenotype. It is possible that the *snrk1α1*-3 mutation causes a subtle decrease in miR156 expression levels (**Figure 3.2.B**), which *per se* is not sufficient to influence the flowering time, but potentially is high enough to cause visible differences in a background where *AP2-like* genes translational repression is compromised, as in the case of *ago1-27*. To confirm this, and given that the WT plants flower earlier, it would be interesting in the future to measure the mature miR156 levels and the *AP2* transcript levels of all the genotypes used for this assay by day 25 and evaluate the differences between them. Nevertheless, as mentioned above, several pathways control the flowering onset, thus it is possible that manipulating AGO1 and SnRK1 may affect other regulatory mechanisms.

Table 1.2. Summarised phenotypic characterisation of flowering under normal long day conditions. Comparative table of the number of days to flowering and the number of rosette leaves between wild type, *ago1-27*, *snrk1α1-3*, *snrk1α1-3* x *ago1-27*, SnRK1α1OE and SnRK1α1OE x *ago1-27* mutants. One minus symbol represents phenotypes with no significant differences in the flowering time for the respective criteria to which they correspond; the plus symbol stands for more; two minus symbols stand for less.

	Flowering	
	days to flowering	rosette leaf number
WT	−	−
SnRK1α1 OE	−	−
ago1-27	+ +	−
SnRK1α1 OE x ago1-27	+ +	−
snrk1α1-3	−	−
snrk1α1-3 x ago1-27	+	− −

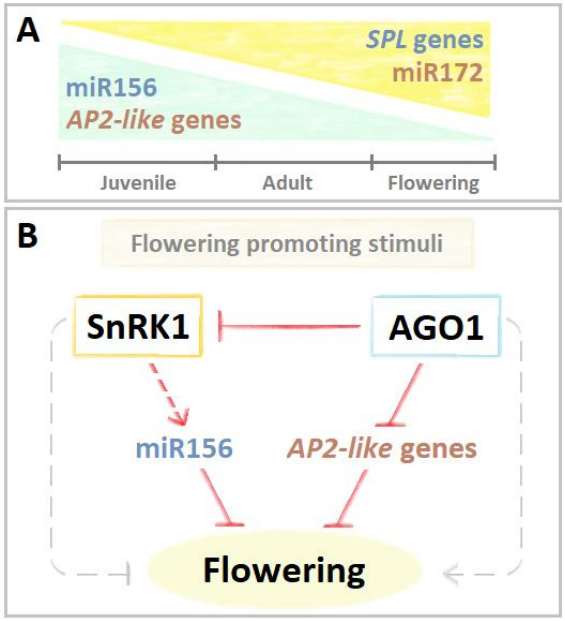

Figure 3.2. AGO1 is a negative regulator of SnRK1 during flowering A) Opposite variation of the expression levels of miR156, miR172 and their target genes during plant development. **B)** Schematic model for the mode of action of SnRK1 and AGO1 during flowering time. Grey dashed lines represent unknown mechanisms.

Finally, to explore the functional interaction between SnRK1 and AGO1 in the future, I developed genetic resources and optimised an experimental setup based on a *SUC::SUL* reporter line, as explained in **Figures 2.8** and **2.9**. In the *SUC::SUL* reporter system[79], the expression of a dsRNA of the *SULPHUR* gene (*SUL*) is expressed under control of the *SUC2* promoter leading to the formation of short interfering RNAs against *SUL* mRNA in phloem companion cells[92] that are loaded into AGO1. As a result, *SUC::SUL* plants display reduced levels of Mg^{2+} chelatase, which is essential for chlorophyll biosynthesis, causing the chlorosis of the silenced cells in the vasculature. Bearing in mind that lower levels of chlorophyll and lower levels of *SUL* transcript are compatible with an enhanced silencing effect, we crossed *sesquiα* mutants with *SUC::SUL* plants to test whether reduced SnRK1 activity affects AGO1-mediated silencing. Under these conditions, one can envision at least two opposite scenarios. If the *sesquiα* mutants have more chlorophyll content and higher levels of *SUL* transcript, it could possibly mean that SnRK1 is indeed a positive regulator of AGO1 activity; whereas if the *sesquiα* mutants have less chlorophyll content and reduced levels of *SUL* transcript, it could

suggest that SnRK1 represses AGO1 activity. If so, a mechanism involving the manipulation of miR168 levels, similar to that of the ABA, could be invoked to explain this negative regulation of AGO1 by SnRK1. In the future, it would be interesting to measure through qRT-PCR the levels of miR168 in the SnRK1 mutants to address this possible negative feedback loop. Alternatively, SnRK1 could repress RISC activity through direct phosphorylation of AGO1 or other RISC component.

Overall, the genetic interaction between SnRK1 and AGO1 seems to support a role for AGO1 as a negative regulator of SnRK1 both in early seedling development and during flowering, although some of the results (glucose phenotypes) suggest additionally a negative regulation of AGO1 by SnRK1. Future work, based on the *SUC::SUL* reporter system described in the Results section, should be conducted to address if the functional interaction between the two proteins supports further these findings or, on the contrary, if the mechanism of choice under these conditions is supportive of our initial hypothesis that SnRK1 is controlling AGO1 activity.

V. CONCLUSIONS

To restore homeostasis and allow plant survival under stress situations, SnRK1 implements vast metabolic and transcriptional changes through mechanisms mostly still unknown. Previous studies have shown that, in response to energy deprivation, miRNAs mediate the repression of specific mRNAs by SnRK1, yet the mechanisms connecting the two pathways remained unclear. Therefore, the work presented on this thesis aimed at addressing two non-mutually exclusive hypotheses: a) SnRK1 affects miRNA biogenesis and b) SnRK1 influences miRNA activity.

Based on gene expression analyses of two specific miRNAs, miR156 and miR319, I found that the partial inactivation of SnRK1 resulted in deficient accumulation of the mature miRNAs tested. Even if it is premature to state that SnRK1 affects miRNA biogenesis, further studies should be conducted to address whether this deficiency is part of a general mechanism or specific just for a subset of miRNAs. In any case, if this deficiency is confirmed in future studies, in addition to mature miRNAs also pri-miRNA levels should be quantified and the interaction between SnRK1 and components of the miRNA biogenesis machinery, such as SE and HYL1, should be investigated.

On the other hand, SnRK1 may additionally influence miRNA activity through AGO1, the final effector of the miRNA pathway. Using a pairwise Y2H assay, I was able to uncover a physical interaction between SnRK1α1 and AGO1. Moreover, the genetic interaction between loss- and gain-of-function SnRK1 mutants and *ago1-27* unveiled a possible scenario in which SnRK1α1 and AGO1 negatively regulate each other during early seedling development and flowering. It would be important in the future to address if the functional interaction between the two proteins further supports these findings.

Taken together, the results described here provide novel evidence that SnRK1 may modulate the miRNA pathway at different levels to control growth, development and plant stress responses. Despite these new findings, many questions remain unanswered and further work will be required to decipher the extent and mechanisms through which SnRK1 impacts on miRNA biogenesis and to dissect the details of its interaction with AGO1.

VI. REFERENCES

1. Bray, E. A., Bailey-Serres, J., and Weretilnyk, E. *Responses to abiotic stresses*. (American Society of Plant Physiologists, 2000).

2. Shi, H., Ishitani, M., Kim, C. & Zhu, J. K. The Arabidopsis thaliana salt tolerance gene *SOS1* encodes a putative Na^+/H^+ antiporter. *Proc. Natl. Acad. Sci. U. S. A.* **97,** 6896–6901 (2000).

3. Drew, M. C., He, C. J. & Morgan, P. W. Programmed cell death and aerenchyma formation in roots. *Trends in Plant Science* **5**, 123-127 (2000).

4. Baena-González, E. Energy signaling in the regulation of gene expression during stress. *Mol. Plant* **3,** 300–313 (2010).

5. Lastdrager, J., Hanson, J. & Smeekens, S. Sugar signals and the control of plant growth and development. *J. Exp. Bot.* **65,** 799–807 (2014).

6. De Block, M. & Van Lijsebettens, M. Energy efficiency and energy homeostasis as genetic and epigenetic components of plant performance and crop productivity. *Curr Opin Plant Biol.* **14,** 275–282 (2011).

7. Baena-González, E., Rolland, F., M. Thevelein, J. & Sheen, J. A central integrator of transcription networks in plant stress and energy signalling. *Nature* **448,** 938–942 (2007).

8. Baena-González, E. & Sheen, J. Convergent energy and stress signaling. *Trends Plant Sci.* **13,** 474–482 (2008).

9. Margalha, L., Valerio, C. & Baena-González, E. Plant SnRK1 Kinases: Structure, Regulation, and Function. 403–438 (2016). doi:10.1007/978-3-319-43589-3_17

10. Polge, C. & Thomas, M. SNF1/AMPK/SnRK1 kinases, global regulators at the heart of energy control? *Trends Plant Sci.* **12,** 20–28 (2007).

11. Crozet, P., Margalha, L., Confraria, A., Rodrigues, A., Martinho, C., Adamo, M., Elias, C. A. & Baena-González, E. Mechanisms of regulation of SNF1/AMPK/SnRK1 protein kinases. *Front. Plant Sci.* **5,** 1–17 (2014).

12. Pierre, M., Traverso, A. J., Boisson, B., Domenichini, S., Bouchez, D., Giglione, C. & Meinnel, T. N-Myristoylation Regulates the SnRK1 Pathway in Arabidopsis. **19,** 2804–2821 (2007).

13. Oakhill, J. S., Chen, Z. P., Scott, J. W., Steel, R., Castelli, L. A., Ling, N., Macaulay, S. L. & Kemp, B. E. β -Subunit myristoylation is the gatekeeper for initiating metabolic stress sensing by AMP-activated protein kinase (AMPK). *Proc. Natl. Acad. Sci.* **107**, 19237-19241 (2010).

14. Oakhill, J. S., Steel, R., Chen, Z. P., Scott, J. W., Ling, N., Tam, S. & Kemp, B. E. AMPK is a direct adenylate charge-regulated protein kinase. *Science* **332**, 1433-1435 (2011).

15. Ramon, M., Ruelens, P., Li, Y, Sheen, J., Geuten, K. & Rolland, F. The hybrid Four-CBS-Domain KINβγ subunit functions as the canonical γ subunit of the plant energy sensor SnRK1. *Plant J.* **75**, 11-25 (2013).

16. Emanuelle, S., Hossain, M. I., Moller, I. E., Pedersen, H. L., van de Meene, A. M., Doblin, M. S., Koay, A., Oakhill, J. S., Scott, J. W., Willats, W. G., Kemp, B. E., Bacic, A., Gooley, P. R. & Stapleton, D. I. SnRK1 from Arabidopsis thaliana is an atypical AMPK. *Plant J.* **82**, 183-192 (2015).

17. Fragoso, S. Espíndula, L, Paéz-Valencia, J., Gamboa, A., Camacho, Y., Martínez-Barajas, E. &

Coelho, P. SnRK1 Isoforms AKIN10 and AKIN11 Are Differentially Regulated in Arabidopsis Plants under Phosphate Starvation. *Plant Physiol.* **149,** 1906–1916 (2009).

18. Radchuk, R., Radchuk, V., Weschke, W., Borisjuk, L & Weber, H. Repressing the Expression of the SUCROSE NONFERMENTING-1-RELATED PROTEIN KINASE Gene in Pea Embryo Causes Pleiotropic Defects of Maturation Similar to an Abscisic Acid-Insensitive Phenotype. *Plant Physiol.* **140,** 263–278 (2005).

19. Zhang, Y., Shewry, P. R., Jones, H., Barcelo, P., Lazzeri, P. A. & Halford, N. G. Expression of antisense SnRK1 protein kinase sequence causes abnormal pollen development and male sterility in transgenic barley. *Plant J.* **28,** 431–441 (2001).

20. Lovas, Á., Bimbó, A., Szabó, L. & Bánfalvi, Z. Antisense repression of StubGAL83 affects root and tuber development in potato. *Plant J.* **33,** 139–147 (2003).

21. Baena-González, E. & Hanson, J. Shaping plant development through the SnRK1–TOR metabolic regulators. *Current Opinion in Plant Biology* **35**, 152-157 (2017).

22. Chen, L., Su, Z.-Z., Huang, L., Xia, F.-N., Qi, H., Xie, L.-J., Xiao, S. & Chen, Q.-F. The AMP-Activated Protein Kinase KIN10 Is Involved in the Regulation of Autophagy in Arabidopsis. *Front. Plant Sci.* **8**, 1201 (2017).

23. Zhang, Y., Primavesi, L. F., Jhurreea, D., Andralojc, P. J., Mitchell, R. A. C., Powers, J. S., Schluepmann, H., Delatte, T., Wingler, A. & Paul, M. J. Inhibition of SNF1-Related Protein Kinase1 Activity and Regulation of Metabolic Pathways by Trehalose-6-Phosphate. *Plant Physiol.* **149,** 1860–1871 (2009).

24. Nunes, C., Primavesi, L. F., Patel, M. K., Martinez-Barajas, E., Powers, S. J., Sagar, R., Fevereiro, P. S., Davis, B. G. & Paul, M. J. Inhibition of SnRK1 by metabolites: Tissue-dependent effects and cooperative inhibition by glucose 1-phosphate in combination with trehalose 6-phosphate. *Plant Physiol. Biochem.* **63,** 89–98 (2013).

25. Kim, G. D., Cho, Y. H. & Yoo, S. D. Phytohormone ethylene-responsive Arabidopsis organ growth under light is in the fine regulation of Photosystem II deficiency-inducible AKIN10 expression. *Sci. Rep.* **7**, 2767 (2017).

26. Im, J. H., Cho, Y. W., Kim, G. D., Kang, G. H., Hong, J. W. & Yoo, S. D. Inverse modulation of the energy sensor Snf1-related protein kinase 1 on hypoxia adaptation and salt stress tolerance in Arabidopsis thaliana. *Plant, Cell Environ.* **37**, 2303-2312 (2014).

27. Jossier, M., Bouly, J. P., Meimoun, P., Arjmand, A., Lessard, P., Hawley, S., Grahame Hardie, D. & Thomas, M. SnRK1 (SNF1-related kinase 1) has a central role in sugar and ABA signalling in Arabidopsis thaliana. *Plant J.* **59,** 316–328 (2009).

28. Rodrigues, A., Adamo, M., Crozet, P., Margalha, L., Confraria, A., Martinho, C., Elias, A., Rabissi, A., Lumbreras, V., González-Guzmán, M., Antoni, R., Rodriguez, P. L. & Baena-González, E. ABI1 and PP2CA Phosphatases Are Negative Regulators of Snf1-Related Protein Kinase1 Signaling in Arabidopsis. *Plant Cell* **25**, 3871-3884 (2013).

29. Sugden, C., Donaghy, P. G., Halford, N. G. & Hardie, D. G. Two SNF1-Related Protein Kinases from Spinach Leaf Phosphorylate and Inactivate 3-Hydroxy-3-Methylglutaryl-Coenzyme A Reductase, Nitrate Reductase, and Sucrose Phosphate Synthase in Vitro. *Plant Physiol.* **120,** 257–274 (1999).

30. Nukarinen, E., Nägele, T., Pedrotti, L., Wurzinger, B., Mair, A., Landgraf, R., Börnke, F., Hanson, J., Teige, M., Baena-González, E., Dröge-Laser, W. & Weckwerth, W. Quantitative phosphoproteomics reveals the role of the AMPK plant ortholog SnRK1 as a metabolic master regulator under energy deprivation. *Sci. Rep.* **6,** 1–19 (2016).

31. Kulma, A., Villadsen, D., Campbell, D. G., Meek, S. E., Harthill, J. E., Nielsen, T. H. & Mackintosh, C. Phosphorylation and 14-3-3 binding of Arabidopsis 6-phosphofructo-2-kinase/ fructose-2,6-bisphosphatase. *Plant J.* **37,** 654–667 (2004).

32. Harthill, J. E., Meek, S. E., Morrice, N., Peggie, M. W., Borch, J., Wong B. W. & Mackintosh, C. Phosphorylation and 14-3-3 binding of Arabidopsis trehalose-phosphate synthase 5 in response to 2-deoxyglucose. *Plant J.* **47,** 211–223 (2006).

33. Mair, A., Pedrotti, L., Wurzinger, B., Anrather, D., Simeunovic, A., Weiste, C., Valerio, C., Dietrick, K. & Kirchler T. SnRK1-triggered switch of bZIP63 dimerization mediates the low-energy response in plants. *Elife* **4**, e05828 (2015).

34. Dröge-Laser, W. & Weiste, C. The C/S1bZIP Network: A Regulatory Hub Orchestrating Plant Energy Homeostasis. *Trends in Plant Science* **23**, 422-433 (2018).

35. Li, S., Castillo-González, C., Yu, B. & Zhang, X. The functions of plant small RNAs in development and in stress responses. *Plant J.* **90,** 654–670 (2017).

36. Confraria, A., Martinho, C., Elias, A., Rubio-Somoza, I. & Baena-González, E. miRNAs mediate SnRK1-dependent energy signaling in Arabidopsis. *Front. Plant Sci.* **4,** (2013).

37. Yu, Y., Jia, T. & Chen, X. The 'how' and 'where' of plant microRNAs. **216,** 1002–1017 (2017).

38. Lee, Y., Kim, M., Han, J., Yeom, K.-H., Lee, S., Baek, S. H. & Kim, V. N. MicroRNA genes are transcribed by RNA polymerase II. *EMBO J.* **23**, 4051-4060 (2004).

39. Achkar, N. P., Cambiagno, D. A. & Manavella, P. A. miRNA Biogenesis: A Dynamic Pathway. *Trends in Plant Science* **21**, 1034-1044 (2016).

40. Yu, B., Yang, Z., Li, J., Minakhina, S., Yang, M., Padgett, R. W., Steward, R. & Chen, X. Methylation as a crucial step in plant microRNA biogenesis. *Science* **307**, 932-935 (2005).

41. Bologna, N. G., Iselin, R., Abriata, L. A., Sarazin, A., Pumplin, N., Jay, F., Grentzinger, T., Dal Peraro, M. & Voinnet, O. Nucleo-cytosolic Shuttling of ARGONAUTE1 Prompts a Revised Model of the Plant MicroRNA Pathway. *Mol. Cell* **69,** 709–719.e5 (2018).

42. Llave, C., Xie, Z., Kasschau, K. D. & Carrington, J. C. Cleavage of Scarecrow-like mRNA targets directed by a class of Arabidopsis miRNA. *Science* **297**, 2053-2056 (2002).

43. Rhoades, M. W., Reinhart, B. J., Lim, L. P., Burge, C. B., Bartel, B. & Bartel, D. P. Prediction of plant microRNA targets. *Cell* **110**, 513-520 (2002).

44. Tang, G., Reinhart, B. J., Bartel, D. P. & Zamore, P. D. A biochemical framework for RNA silencing in plants. *Genes Dev.* **17**, 49-63 (2003).

45. Aukerman, M. J., Sakai, H. Regulation of Flowering Time and Floral Organ Identity by a MicroRNA and Its APETALA2-Like Target Genes. *Plant Cell* **15**, 2730-2741 (2003).

46. Chen, X. A MicroRNA as a Translational Repressor of APETALA2 in Arabidopsis Flower Development. *Science* **303**, 2022-2025 (2004).

47. Gandikota, M., Birkenbihl, R. P., Höhmann, S., Cardon, G. H., Saedler, H. & Huijser, P. The miRNA156/157 recognition element in the 3' UTR of the Arabidopsis SBP box gene SPL3 prevents early flowering by translational inhibition in seedlings. *Plant J.* **49,** 683–693 (2007).

48. Brodersen, P., Sakvarelidze-Achard, L., Bruun-Rasmussen, M., Dunoyer, P., Yamamoto, Y. Y., Sieburth, L. & Voinnet O. Widespread translational inhibition by plant miRNAs and

siRNAs. *Science* **320**, 1185-1190 (2008).

49. Li, S., Liu, L., Zhuang, X., Yu, Y., Liu, X., Cui, X., Ji, L., Pan, Z., Cao, X., Mo, B., Zhang, F., Raikhel, N., Jiang, L. & Chen, X. MicroRNAs inhibit the translation of target mRNAs on the endoplasmic reticulum in arabidopsis. *Cell* **153**, 562-574 (2013).

50. Oliver, C., Pradillo, M., Jover-Gil, S., Cuñado, N., Ponce, M. R. & Santos, J. L. Loss of function of Arabidopsis microRNA-machinery genes impairs fertility, and has effects on homologous recombination and meiotic chromatin dynamics. *Sci. Rep.* **7**, 9280 (2017).

51. Schauer, S. E., Jacobsen, S. E., Meinke, D. W. & Ray, A. DICER-LIKE1: Blind men and elephants in Arabidopsis development. *Trends in Plant Science* **7**, 487-491 (2002).

52. Vazquez, F., Gasciolli, V., Crété, P. & Vaucheret, H. The nuclear dsRNA binding protein HYL1 is required for microRNA accumulation and plant development, but not posttranscriptional transgene silencing. *Curr. Biol.* **14**, 346-351 (2004).

53. Teotia, S. & Tang, G. To bloom or not to bloom: Role of micrornas in plant flowering. *Mol. Plant* **8,** 359–377 (2015).

54. Koyama, T., Sato, F. & Ohme-Takagi, M. Roles of miR319 and TCP transcription factors in leaf development. *Plant Physiol.* **175**, 874-885 (2017).

55. Reyes, J. L. & Chua, N. H. ABA induction of miR159 controls transcript levels of two MYB factors during Arabidopsis seed germination. *Plant J.* **49,** 592–606 (2007).

56. Rodriguez, R. E., Mecchia, M. A., Debernardi, J. M., Schommer, C., Weigel, D. & Palatnik, J. F. Control of cell proliferation in Arabidopsis thaliana by microRNA miR396. *Development* **137**, 103, 112 (2010).

57. Wang, J., Meng, X., Dobrovolskaya, O. B., Orlov, Y. L. & Chen, M. Non-coding RNAs and Their Roles in Stress Response in Plants Wang J et al / miRNA and lncRNA in Plant Stress Response. *Genomics, Proteomics Bioinforma.* **15,** 301–312 (2017).

58. Lin, J.-S., Kuo, C. C., Yang, I.-C., Tsai, W.-A., Shen, Y.-H., Lin, C.-C., Liang, Y.-C., Li, Y.-C., Kuo, Y.-W., King, Y.-C., Lai, H.-M. & Jeng, S.-T. MicroRNA160 Modulates Plant Development and Heat Shock Protein Gene Expression to Mediate Heat Tolerance in Arabidopsis. *Front. Plant Sci.* **9,** 1–16 (2018).

59. Tian, X., Song, L., Wang, Y., Jin, W., Tong, F. & Wu, F. miR394 Acts as a Negative Regulator of Arabidopsis Resistance to B. cinerea Infection by Targeting LCR. *Front. Plant Sci.* **9,** 1–11 (2018).

60. Xu, M. Y., Zhang, L., Li, W. W., Hu, X. L., Wang, M. B., Fan, Y. L., Zhang, C. Y. & Wang, L. Stress-induced early flowering is mediated by miR169 in Arabidopsis thaliana. *J. Exp. Bot.* **65**, 89-101 (2014).

61. Li, W.-X., Oono, Y., Zhu, J., He, X. J., Wu, J. M., Iida, K., Lu, X. Y., Cui, X., Jin, H. & Zhu, J. K. The Arabidopsis NFYA5 Transcription Factor Is Regulated Transcriptionally and Posttranscriptionally to Promote Drought Resistance. *Plant Cell* **20**, 2238-2251 (2008).

62. Akdogan, G., Tufekci, E. D., Uranbey, S. & Unver, T. miRNA-based drought regulation in wheat. *Funct. Integr. Genomics* **16**, 221-233 (2016).

63. Lu, C. & Fedoroff, N. A Mutation in the Arabidopsis HYL1 Gene Encoding a dsRNA Binding Protein Affects Responses to Abscisic Acid, Auxin, and Cytokinin. *Plant Cell* **12**, 2351-2366 (2000).

64. Kim, S., Yang, J. Y., Xu, J., Jang, I. C., Prigge, M. J. & Chua, N. H. Two cap-binding proteins CBP20 and CBP80 are involved in processing primary microRNAs. *Plant Cell Physiol.* **49**, 1634-1644 (2008).

65. Zhang, J. F., Yuan, L. J., Shao, Y., Du, W., Yan, D. W. & Lu, Y. T. The disturbance of small RNA pathways enhanced abscisic acid response and multiple stress responses in Arabidopsis. *Plant, Cell Environ.* **31**, 562-574 (2008).

66. Li, W., Cui, X., Meng, Z., Huang, X., Xie, Q., Wu, H., Jin, H., Zhang, D. & Liang, W. Transcriptional Regulation of Arabidopsis MIR168a and ARGONAUTE1 Homeostasis in Abscisic Acid and Abiotic Stress Responses. *Plant Physiol.* **158**, 1279-1292 (2012).

67. Dolata, J., Taube, M., Bajczyk, M., Jarmolowski, A., Szweykowska-Kulińska, Z. & Bielewicz, D. Regulation of Plant Microprocessor Function in Shaping microRNA Landscape. *Front. Plant Sci.* **9**, 753 (2018).

68. Vaucheret, H. Plant ARGONAUTES. *Trends in Plant Science* **13**, 350-358 (2008).

69. Thieme, C. J., Schudoma, C., May, P. & Walther, D. Give It AGO: The Search for miRNA-Argonaute Sorting Signals in Arabidopsis thaliana Indicates a Relevance of Sequence Positions Other than the 5′-Position Alone. *Front. Plant Sci.* **3**, 272 (2012).

70. Fang, X. & Qi, Y. RNAi in Plants: An Argonaute-Centered View. *Plant Cell* **28**, 272-285 (2016).

71. Mi, S., Cai, T., Hu, Y., Chen, Y., Hodges, E., Ni, F., Wu, L., Li, S., Zhou, H., Long, C., Chen, S., Hannon, G. J. & Qi, Y. Sorting of Small RNAs into Arabidopsis Argonaute Complexes Is Directed by the 5′ Terminal Nucleotide. *Cell* **133**, 116-127 (2008).

72. Takeda, A., Iwasaki, S., Watanabe, T., Utsumi, M. & Watanabe, Y. The mechanism selecting the guide strand from small RNA duplexes is different among Argonaute proteins. *Plant Cell Physiol.* **49**, 493-500 (2008).

73. Kim, V. N. Sorting Out Small RNAs. *Cell* **133**, 25-26(2008).

74. Baumberger, N. & Baulcombe, D. C. Arabidopsis ARGONAUTE1 is an RNA Slicer that selectively recruits microRNAs and short interfering RNAs. *Proc. Natl. Acad. Sci.* **102**, 11928-11933 (2005).

75. Vaucheret, H., Mallory, A. C. & Bartel, D. P. AGO1 Homeostasis Entails Coexpression of MIR168 and AGO1 and Preferential Stabilization of miR168 by AGO1. *Mol. Cell* **22**, 129-136 (2006).

76. Liu, C., Xin, Y., Xu, L., Cai, Z., Xue, Y., Liu, Y., Xie, D., Liu, Y. & Qi, Y. Arabidopsis ARGONAUTE 1 Binds Chromatin to Promote Gene Transcription in Response to Hormones and Stresses. *Dev. Cell* **44,** 348–361.e7 (2018).

77. Jeong, E. Y., Seo, P. J., Woo, J. C. & Park, C. M. AKIN10 delays flowering by inactivating IDD8 transcription factor through protein phosphorylation in Arabidopsis. *BMC Plant Biol.* **15**, 110 (2015)

78. Morel, J., Godon, C., Mourrain, P., Feuerbach, F. & Proux, F. Fertile Hypomorphic. *Society* **14,** 629–639 (2002).

79. Himber, C., Dunoyer, P., Moissiard, G., Ritzenthaler, C. & Voinnet, O. Transitivity-dependent and -independent cell-to-cell movement of RNA silencing. *EMBO J.* **22**, 4523-4533 (2003).

80. Dunoyer, P., Himber, C. & Voinnet, O. DICER-LIKE 4 is required for RNA interference and

produces the 21-nucleotide small interfering RNA component of the plant cell-to-cell silencing signal. *Nat. Genet.* **37**, 1356-1360 (2005).

81. Kramer, M. F. Stem-loop RT-qPCR for miRNAs. *Curr. Protoc. Mol. Biol.* Chapter 15, Unit 15:10 (2011).

82. Livak, K. J. & Schmittgen, T. D. Analysis of relative gene expression data using real-time quantitative PCR and the 2-ΔΔCT method. *Methods* **25**, 402-408 (2001).

83. Vandesompele, J., De Preter, K., Pattyn, F., Poppe, B., Van Roy, N., De Paepe, A. & Speleman, F. Accurate normalization of real-time quantitative RT-PCR data by geometric averaging of multiple internal control genes. *Genome Biol.* **3**, Research0034 (2002).

84. Laemmli, U. K. Cleavage of structural proteins during the assembly of the head of bacteriophage T4. *Nature* **227**, 680-685 (1970).

85. Ni, Z., Kim, E. D., Ha, M., Lackey, E., Liu, J., Zhang, Y., Sun, Q. & Chen, Z. J. Altered circadian rhythms regulate growth vigour in hybrids and allopolyploids. *Nature* **457**, 327-331 (2009).

86. Wang, J. W. Regulation of flowering time by the miR156-mediated age pathway. *Journal of Experimental Botany* **65**, 4723-4730 (2014).

87. Yan, J., Wang, P., Wang, D., Hsu, C.-C., Tang, K., Zhang, H., Hou, Y.-J., Zhao, Y., Wang, Q., Zhao, C., Zhu, X., Tao, W. A., Li, J. & Zhu, J.-K. The SnRK2 kinases modulate miRNA accumulation in Arabidopsis. *PLoS Genet.* **13,** 1–21 (2017).

88. Duarte, G. T., Matiolli, C. C., Pant, B. D., Schlereth, A., Scheible, W.-R., Stitt, M., Vicentini, R. & Vincentz, M. Involvement of microRNA-related regulatory pathways in the glucose-mediated control of Arabidopsis early seedling development. *J. Exp. Bot.* **64,** 4301–4312 (2013).

89. Tsai, A. Y. L. & Gazzarrini, S. AKIN10 and FUSCA3 interact to control lateral organ development and phase transitions in Arabidopsis. *Plant J.* **69**, 809-821 (2012).

90. Earley, K., Smith, M. R., Weber, R., Gregory, B. D. & Poethig, R. S. An endogenous F-box protein regulates ARGONAUTE1 in Arabidopsis thaliana. *Silence* **1**, 15 (2010).

91. Vaucheret, H., Vazquez, F., Crété, P. & Bartel, D. P. The action of ARGONAUTE1 in the miRNA pathway and its regulation by the miRNA pathway are crucial for plant development. *Genes Dev.* **18**, 1187-1197 (2004).

92. Stadler, R. & Sauer, N. The Arabidopsis thaliana AtSUC2 gene is specifically expressed in companion cells. *Bot. Acta* **109**, 261-340 (1996).

93. Dunoyer, P., Himber, C., Ruiz-Ferrer, V., Alioua, A. & Voinnet, O. Intra- and intercellular RNA interference in Arabidopsis thaliana requires components of the microRNA and heterochromatic silencing pathways. *Nat. Genet.* **39**, 848-856 (2007).

94. McNellis, T. W. Light Control of Seedling Morphogenetic Pattern. *Plant Cell Online* **7,** 1749–1761 (1995).

95. Zhou, X. Y., Song, L. & Xue, H. W. Brassinosteroids regulate the differential growth of arabidopsis hypocotyls through auxin signaling components IAA19 and ARF7. *Mol. Plant* **6**, 887- 904 (2013).

96. Dröge-Laser, W., Snoek, B. L., Snel, B. & Weiste, C. The Arabidopsis bZIP transcription factor family — an update. *Current Opinion in Plant Biology* **45**, 36-49 (2018).

97. Von Born, P., Bernardo-Faura, M. & Rubio-Somoza, I. An artificial miRNA system reveals that relative contribution of translational inhibition to miRNA-mediated regulation depends on environmental and developmental factors in Arabidopsis thaliana. *PLoS One* **13**, e019298 (2018).

98. Rogers, K. & Chen, X. Biogenesis, Turnover, and Mode of Action of Plant MicroRNAs. *Plant Cell* **25,** 2383–2399 (2013).

99. Wu, G. & Poethig, R. S. Temporal regulation of shoot development in Arabidopsis thaliana by miR156 and its target SPL3. *Development* **133**, 3539-3547 (2006).

100. Cui, L. G., Shan, J. X., Shi, M., Gao, J. P. & Lin, H. X. The miR156-SPL9-DFR pathway coordinates the relationship between development and abiotic stress tolerance in plants. *Plant J.* **80**, 1108-1117 (2014).

101. Yang, L., Xu, M., Koo, Y., He, J. & Scott Poethig, R. Sugar promotes vegetative phase change in Arabidopsis thaliana by repressing the expression of MIR156A and MIR156C. *Elife* **2**, e00260 (2013).

102. Yu, S., Cao, L., Zhou, C.-M., Zhang, T.-Q., Lian, H., Sun, Y., Wu, J., Huang, J., Wang, G. & Wang, J.-W. Sugar is an endogenous cue for juvenile-to-adult phase transition in plants. *Elife* **2**, e00269 (2013).

103. Uberti Manassero, N. G., Viola, I. L., Welchen, E. & Gonzalez, D. H. TCP transcription factors: Architectures of plant form. *Biomolecular Concepts* **4**, 111-127 (2013).

104. Kieffer, M., Master, V., Waites, R. & Davies, B. TCP14 and TCP15 affect internode length and leaf shape in Arabidopsis. *Plant J.* **68**, 147-158 (2011).

105. Mao, Y., Wu, F., Yu, X., Bai, J., Zhong, W. & He, Y. microRNA319a-Targeted Brassica rapa ssp. pekinensis TCP Genes Modulate Head Shape in Chinese Cabbage by Differential Cell Division Arrest in Leaf Regions. *Plant Physiol.* **164**, 710-720 (2014).

106. Danisman S., van der Wal, F., Dhondt, S., Waites, R., de Folter, S., Bimbo, A., van Dijk, A. D., Muino, J. M., Cutri, L., Dornelas, M. C., Angenent, G. C. & Immink, R. G. Arabidopsis Class I and Class II TCP Transcription Factors Regulate Jasmonic Acid Metabolism and Leaf Development Antagonistically. *Plant Physiol.* **159**, 1511-1523 (2012).

107. Resentini, F., Felipo-Benavent, A., Colombo, L., Blázquez, M. A., Alabadi, D. & Masiero, S. TCP14 and TCP15 mediate the promotion of seed germination by gibberellins in arabidopsis thaliana. *Molecular Plant* **8**, 482-485 (2015).

108. Aguilar-Martinez, J. A., Poza-Carrion, C. & Cubas, P. Arabidopsis BRANCHED1 Acts as an Integrator of Branching Signals within Axillary Buds. *PLANT CELL ONLINE* **19**, 458-472 (2007).

109. Zhou, M., Li, D., Li, Z., Hu, Q., Yang, C., Zhu, L. & Luo, H. Constitutive Expression of a miR319 Gene Alters Plant Development and Enhances Salt and Drought Tolerance in Transgenic Creeping Bentgrass. *Plant Physiol.* **161**, 1375-1391 (2013).

110. Danisman, S. TCP Transcription Factors at the Interface between Environmental Challenges and the Plant's Growth Responses. *Front. Plant Sci.* **7**, 1930 (2016).

111. Mukhopadhyay, P. & Tyagi, A. K. OsTCP19 influences developmental and abiotic stress signaling by modulating ABI4-mediated pathways. *Sci. Rep.* **5**, 9998 (2015).

112. Giraud, E., Ng, S., Carrie, C., Duncan, O., Low, J., Lee, C. P., Aken, O. V., Millar, A. H., Murcha, M. & Whelan, J. TCP Transcription Factors Link the Regulation of Genes Encoding

Mitochondrial Proteins with the Circadian Clock in *Arabidopsis thaliana*. *Plant Cell* **22**, 3921-3934 (2010).

113. Arribas-Hernández, L., Kielpinski, L. J. & Brodersen, P. mRNA decay of most Arabidopsis miRNA targets requires slicer activity of AGO1. *Plant Physiol.* **171,** pp.00231.2016 (2016).

114. Iki, T., Yoshikawa, M., Meshi, T. & Ishikawa, M. Cyclophilin 40 facilitates HSP90-mediated RISC assembly in plants. *EMBO J.* **31**, 267-278 (2012).

115. Wang, W., Ye, R., Xin, Y., Fang, X., Li, C., Shi, H., Zhou, X. & Qi, Y. An Importin β Protein Negatively Regulates MicroRNA Activity in Arabidopsis. *Plant Cell* **23**, 3565-3576 (2011).

116. Cui, Y., Fang, X. & Qi, Y. TRANSPORTIN1 Promotes the Association of MicroRNA with ARGONAUTE1 in Arabidopsis. *Plant Cell* **28**, 2576-2585 (2016).

117. Derrien, B., Baumberger, N., Schepetilnikov, M., Viotti, C., De Cillia, J., Ziegler-Graff, V., Isono, E., Schumacher, K. & Genschik, P. Degradation of the antiviral component ARGONAUTE1 by the autophagy pathway. *Proc. Natl. Acad. Sci.* **109**, 15942-15946 (2012).

118. Soto-Burgos, J. & Bassham, D. C. SnRK1 activates autophagy via the TOR signaling pathway in Arabidopsis thaliana. *PLoS One* **12,** 1–19 (2017).

119. Qi, H. H., Ongusaha, P. P., Myllyharju, J., Cheng, D., Pakkanen, O., Shi, Y., Lee, S. W., Peng, J. & Shi Y. Prolyl 4-hydroxylation regulates Argonaute 2 stability. *Nature* **455**, 421-424 (2008).

120. Zeng, Y., Sankala, H., Zhang, X. & Graves, P. R. Phosphorylation of Argonaute 2 at serine-387 facilitates its localization to processing bodies. *Biochem. J.* **413**, 429-436 (2008).

121. Rudel, S., Wang, Y., Lenobel, R., Körner, R., Hsiao, H.-H., Urlaub, H., Patel, D. & Meister, G. Phosphorylation of human Argonaute proteins affects small RNA binding. *Nucleic Acids Res* **39**, 2330-2343 (2010).

122. Shen, J., Xia, W., Khotskaya, Y. B., Huo, L., Nakanishi, K., Lim, S. O., Du, Y., Wang, Y., Chang, W. C., Chen, C. H., Hsu, J. L., Wu, Y., Lam, Y. C., James, B. P., Liu, X., Liu, C. G., Patel, D. J. & Hung, M. C. EGFR modulates microRNA maturation in response to hypoxia through phosphorylation of AGO2. *Nature* **497**, 383-387 (2013).

123. Horman, S. R., Janas, M. M., Litterst, C., Wang, B., MacRae, I. J., Sever, M. J., Morrissey, D. V., Graves, P., Luo, B., Umesalma, S., Qi, H. H., Miraglia, L. J., Novina, C. D. & Orth, A. P. Akt-mediated phosphorylation of argonaute 2 downregulates cleavage and upregulates translational repression of MicroRNA targets. *Mol. Cell* **50**, 356-367 (2013).

124. Quévillon Huberdeau, M., Zeitler, D. M., Hauptmann, J., Bruckmann, A., Fressigné, L., Danner, J., Piquet, S., Strieder, N., Engelmann, J. C., Jannot, G., Deutzmann, R., Simard, M. J. & Meister, G. Phosphorylation of Argonaute proteins affects mRNA binding and is essential for microRNA-guided gene silencing *in vivo*. *EMBO J.* **36**, 2088-2106 (2017).

125. Golden, R. J., Chen, B., Li, T., Braun, J., Manjunath, H., Chen, X., Wu, J., Schmid, V., Chang, T. C., Kopp, F., Ramirez-Martinez, A., Tagliabracci, V. S., Chen, Z.-J., Xie, Y. & Mendell, J. T. An Argonaute phosphorylation cycle promotes microRNA-mediated silencing. *Nature* **542**, 197-202 (2017).

126. Klepikova, A. V., Kasianov, A. S., Gerasimov, E. S., Logacheva, M. D. & Penin, A. A. A high resolution map of the Arabidopsis thaliana developmental transcriptome based on RNA-seq profiling. *Plant J.* **88**, 1058-1070 (2016).

127. Nambara, E., Hayama, R., Tsuchiya, Y., Nishimura, M., Kawaide, H., Kamiya, Y. & Naito S.

The role of ABI3 and FUS3 loci in Arabidopsis thaliana on phase transition from late embryo development to germination. *Dev. Biol.* **220**, 412-423 (2000).

128. Gazzarrini, S., Tsuchiya, Y., Lumba, S., Okamoto, M. & McCourt, P. The transcription factor FUSCA3 controls developmental timing in Arabidopsis through the hormones Gibberellin and abscisic acid. *Dev. Cell* **7**, 373-385 (2004).

129. Curaba, J., Moritz, T. & Blervaque, R. AtGA3ox2, a key gene responsible for bioactive gibberellin biosynthesis, is regulated during embryogenesis by LEAFY COTYLEDON2 and FUSCA3 in Arabidopsis. *Plant Physiol.* **136**, 3660-3669 (2004).

130. Bitrián, M., Roodbarkelari, F., Horváth, M. & Koncz, C. BAC-recombineering for studying plant gene regulation: Developmental control and cellular localization of SnRK1 kinase subunits. *Plant J.* **65**, 829-842 (2011).

131. Lopez-Molina, L., Mongrand, S. & Chua, N.-H. A postgermination developmental arrest checkpoint is mediated by abscisic acid and requires the ABI5 transcription factor in Arabidopsis. *Proc. Natl. Acad. Sci.* **98**, 4782-4787 (2001).

132. Tognetti, J. A., Pontis, H. G. & Martínez-Noël, G. M. A. Sucrose signaling in plants: A world yet to be explored. *Plant Signaling and Behavior* **8**, e23316 (2013).

133. Jung, J.-H. Seo, Y.-H., Seo, P. J., Reyes, J. L., Yun, J., Chua, N.-H. & Park, C.-M. The GIGANTEA-Regulated MicroRNA172 Mediates Photoperiodic Flowering Independent of CONSTANS in Arabidopsis. *Plant Cell* **19**, 2736-2748 (2007).

134. Wang, J. W., Czech, B. & Weigel, D. miR156-Regulated SPL Transcription Factors Define an Endogenous Flowering Pathway in Arabidopsis thaliana. *Cell* **138**, 738-749 (2009).

135. Kasschau, K. D., Xie, Z., Allen, E., Llave, C., Chapman E. J. Krisan, K. A. & Carrington J. C. P1/HC-Pro, a viral suppressor of RNA silencing, interferes with Arabidopsis development and miRNA function. *Developmental Cell* **4**, 205-217 (2003).

136. Schwab, R. Palatnik, J. F., Riester, M., Schommer, C., Schmid, M. & Weigel D. Specific effects of microRNAs on the plant transcriptome. *Dev. Cell* **8**, 517-527 (2005).

137. Mathieu, J., Yant, L. J., Mürdter, F., Küttner, F. & Schmid, M. Repression of flowering by the miR172 target SMZ. *PLoS Biol.* **7**, e1000148 (2009).

VII. ANNEX

Supplementary Table 1. List of the primers used in this study

Gene Name	Locus ID	Primer Sequence (5' - 3')	Comment	Lab ID
AGO1	AT1G48410	GGGGACAAGTTTGTACAAAAAAGCAGGCT TCATGGTGAGAAAGAGAAGAACGG	Cloning Forward Primer	2383
		GGGGACCACTTTGTACAAGAAAGCTGGGTC GCAGTAGAACATGACACGC	Cloning Reverse Primer	2384
		GTAAAACGACGGCCAG	Sequencing	586
		TCATCAAGGAGGTCGAGGAG	Sequencing	905
		TTTGGAGGGGAAACAATCAG	Sequencing	2392
		CTACCATGCTTGCAAGTTGGG	Sequencing	1156
		CCCTGAGCAAGTAGAGAAGG	Sequencing	1157
		CAGGAAACAGCTATGAC	Sequencing	587
		AGATGGTGCACGATGCACAG	attL sites sequencing	554
		GCCTCCTCTAACGTTCATGA	attL sites sequencing	714
		CCCTGAGCAAGTAGAGAAGG	attL sites sequencing	1157
		TGCAAGATGCACACGCTCAGTTTC	attL sites sequencing	1836
miR156		GTCGTATCCAGTGCAGGGTCCGAGGTATTC GCACTGGATACGACGTGCTC	Stem-loop RT Primer cDNA synthesis	610
		GCGGCGGTGACAGAAGAGAGT	qRT-PCR Fw Primer	611
miR319		GTCGTATCCAGTGCAGGGTCCGAGGTATTC GCACTGGATACGACAGGGAG	Stem-loop RT Primer cDNA synthesis	2440
		CGCCGTTGGACTGAAGGGAG	qRT-PCR Fw Primer	2462
		$Oligo(dT)_{18}$	cDNA synthesis	
		GTGCAGGGTCCGAGGT	Universal qRT-PCR	614
EIF4	AT3G13920	TCATAGATCTGGTCCTTAAACC	qRT-PCR Ref. Gene Fw	334
		GGCAGTCTCTTCGTGCTGAC	qRT-PCR Ref. Gene Rv	335
UBQ10	AT4G05320	GGCCTTGTATAATCCCTGATGAATAAG	qRT-PCR Ref. Gene Fw	2026
		AAAGAGATAACAGGAACGGAAACATAGT	qRT-PCR Ref. Gene Rv	2027
UBC21		CTGCGACTCAGGGAATCTTCTAA	qRT-PCR Ref. Gene Fw	2089
		TTGTGCCATTGAATTGAACCC	qRT-PCR Ref. Gene Rv	2090
KIN10	AT3G01090	CCAGCATAATAGAGAACGAAGC	Genotyping	374
		ATATTGACCATCATACTCATTGC	Genotyping	722
		TTGACCCATCAAATAATACACGAA	Genotyping	1758
KIN11	AT3G29160	CGTAGTGATCCACATGTGCAG	Genotyping	804
		GATTGCAGACTTTGGGTTGAG	Genotyping	805
		TGCGGTTTGATGATTATAATCG	Genotyping	806
		TCGATTCCACTCCATTATTGC	Genotyping	807
		T-DNA-Wis	Genotyping	808

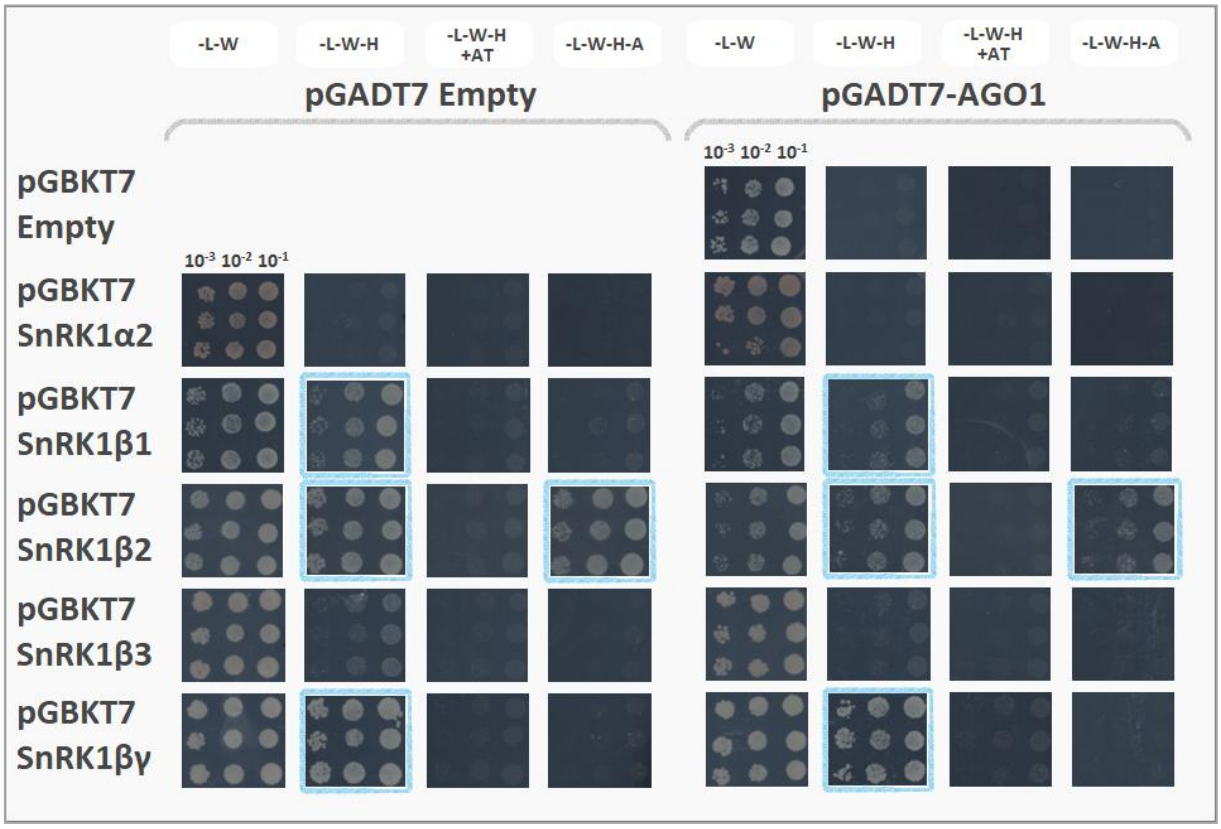

Supplementary Figure 1. SnRK1α2 and β3 do not interact with AGO1 in a pairwise yeast two hybrid assay. Ten-fold serial dilutions of saturated yeast cultures were spotted onto plates containing synthetic dropout medium with increased stringency. 25 mM amino-triazole (AT) was used to increase stringency of -L-W-H medium. Cells co-expressing SnRK1α2 or SnRK1β3 and AGO1 failed to grow in medium with increased stringency. Cells co-expressing SnRK1β1, or β2 or βγ and AGO1 yielded a very high background growth that precluded the assessment of a possible interaction between these subunits and AGO1. This assay was repeated two times with similar results. The picture shows a representative experiment.